NASA Technical Memorandum 78737

# Development of a Nonlinear Switching Function and Its Application to Static Lift Characteristics of Straight Wings



Donald E. Hewes

SEPTEMBER 1978

NASA

NASA Technical Memorandum 78737

# Development of a Nonlinear Switching Function and Its Application to Static Lift Characteristics of Straight Wings

Donald E. Hewes
*Langley Research Center*
*Hampton, Virginia*

National Aeronautics
and Space Administration

**Scientific and Technical
Information Office**

1978

## SUMMARY

Increasing attention is being given to the measurement and mathematical representation of nonlinear aerodynamic coefficients in studies of many dynamic flight problems. In an attempt to overcome some of the complexities involved in handling these nonlinear variables, a simplified method of representing these variables was developed to facilitate the mathematical-modeling process. The method, which employs a curve-fitting technique, utilizes a specially developed mathematical expression as a modulating or switching function. The application of this function to the modeling technique is demonstrated by showing the development of the mathematical models for the static nonlinear lift characteristics, up to an angle of attack of $90^{\circ}$, for a group of straight wings with different airfoil and planform characteristics. The mathematical models are based on the wind-tunnel data for these wings as reported in several references. The empirically determined lift characteristics were matched by the mathematical models within ±4 percent of the maximum values over the complete angle-of-attack range. The application of this technique to other aerodynamic and nonaerodynamic characteristics is discussed briefly.

## INTRODUCTION

Over many years there has been increasing attention given to the measurement and mathematical representation of nonlinear aerodynamic coefficients in studies of many dynamic flight problems of various types of aircraft. Separation of the airflow over propellers, rotors, and surfaces of these aircraft is probably the most common source of these nonlinear coefficients. In the case of analytical and simulation studies of the stall and spin motions of the airplane where the airflow is partially or fully separated over large portions of the airplanes, the measurement and mathematical representation, as well as the subsequent manipulation of the complete set of aerodynamic coefficients, are extremely complex. Because of recent renewed efforts to analyze the stall and spin problems, particularly those of the light-airplane category, an attempt has been made to develop a simplified method for representing these nonlinear characteristics that have been measured. The purpose of the present paper is to discuss the resultant technique that has been applied to the mathematical modeling of the nonlinear lift characteristics of straight wings of the type used on many current general-aviation light airplanes. The coefficients of the model can be estimated fairly easily by inspection of the data curves and simple graphical analysis. The use of a mathematical expression as a modulating or switching function and its application to this technique are discussed. The application of the modulating function to other nonlinear aerodynamic characteristics and to nonaerodynamic problems is also discussed briefly.

## SYMBOLS

$A,B,\ldots,G$ dimensional and nondimensional coefficients used in mathematical-model equations

$C_D$ drag coefficient, $\text{Drag}/qS_w$

$C_L$ lift coefficient, $\text{Lift}/qS_w$

$C_{L,A}, C_{L,B}, C_{L,C}$ components of lift coefficient corresponding to terms in equation (8)

$\bar{c}$ mean geometric chord, m

$m,n$ switching coefficients (switching ratio and shape factor, respectively)

$N_{Re}$ Reynolds number, $\rho V\bar{c}/\mu$

$q$ dynamic pressure, $\frac{1}{2}\rho V^2$, Pa

$R$ switching variable

$\bar{S}$ cutoff switching function (see eq. (4))

$\underline{S}$ cut-on switching function (see eq. (5))

$S_w$ wing area, $m^2$

$V$ free-stream velocity, m/sec

$\alpha$ angle of attack relative to that for zero lift, deg

$\alpha_o$ reference-axis angle of attack for zero lift, deg

$\alpha_1, \alpha_2, \ldots$ specific values of switching points (see eq. (8))

$\beta$ angle of sidelsip of reference axis, deg

$\mu$ air dynamic viscosity, N-sec/m

$\rho$ air density, $kg/m^3$

Subscripts:

max maximum

w wing

## MODELING NONLINEAR CHARACTERISTICS

When attempting to solve dynamic flight problems that involve excursions into the stall region, the engineer is faced not only with a general lack of data covering the large matrix of aerodynamic coefficients involved, but he is faced also with the complexities of manipulating the basically nonlinear data so that they can be effectively employed by using the computational techniques available. Because of the scarcity of data, there is the need to employ methods to interpolate and extrapolate between and beyond the intervals of the available data points. Also, there is the need to use these data to make estimates for those data that are not available. The assembly of the very large quantity of data, both measured and estimated, required for these dynamic flight problems can be tedious, cumbersome, and subject to random errors that are difficult for the engineer to detect.

In the light of these difficulties, therefore, it was considered desirable to be able to convert the original tabular data obtained from the wind-tunnel tests into mathematical models which could be manipulated fairly easily by modern high-speed computers. From the engineers' viewpoint, it was considered desirable to employ terms which could be easily interpreted and which would have some physical significance relative to the flow phenomena involved. Furthermore, the model should permit the engineer to readily change selected coefficients to account for various changes in configuration or flight condition, as well as to isolate the influence of individual aerodynamic terms or components.

## DEVELOPMENT OF MATHEMATICAL MODULATING OR SWITCHING FUNCTION

Before the modeling technique is presented, a discussion of the mathematical modulating function, which is the key element in this technique, is presented.

A modulating function is defined for use herein as a term which changes from the value of 1 to 0, or vice versa, in some prescribed manner as the controlling variable changes its value relative to some reference or operating point. The rapidity with which the function changes value as the operating point is approached is referred to as the gain of the function. A function with a low gain begins to change value at some appreciable distance from the operating point, whereas a high-gain function retains the value of 1 or 0 until the operating point is almost reached. As the gain is increased toward infinity, the function takes on the characteristics of an on-off switch that changes value only at the specific operating point. For convenience, the subject modulating function is referred to simply as a switch, although it may have low-gain characteristics in most applications. The switching function is represented by the symbol S. The subject modulating or switching function is based on the family of exponential equations, two of which are

$$y = e^{-x} \tag{1}$$

and

$$y = e^{-x^2} \tag{2}$$

Equation (1) is used often to represent time variant natural phenomena such as the response of a damped mass-spring system to a step input. Equation (2) is used to represent the probability of occurrence or the normal distribution encountered in many natural phenomena. The only difference between the two equations is the exponential value of $x$. The curves for these two equations are compared in sketch (a), which shows the variation of $y$ for values of $x$ from 0 to 2.

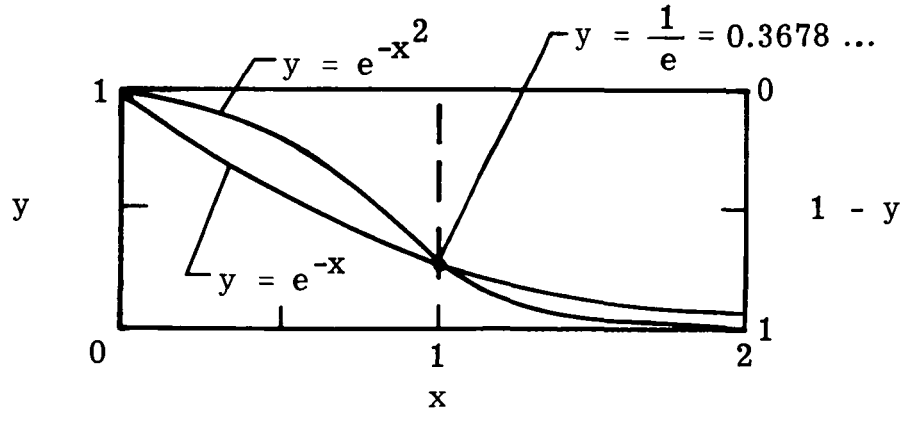


Sketch (a)

Both functions (eqs. (1) and (2)) have the value of 1 when $x = 0$ and approach the value of 0 as $x$ increases beyond the value of 1. The two equations have the characteristics of a low-gain modulating function, as previously described, which switches slowly from "on" to "off" as $x$ increases. Furthermore, both functions have the same value of $y = \frac{1}{e} = 0.3678 \ldots$ at the point where $x = 1$. This point is referred to as the operating point. The difference between the two functions is in the shape of the curves or the rate at which they change or "cut off" as $x$ increases. Thus, it can be seen that the value of the exponent of $x$ determines the shape of the curve and the cutoff or gain characteristics of the switching function. As the value of the exponent of $x$ is increased, the slope of the curve where it passed through $x = 1$ becomes steeper.

The reverse action of the cutoff switching function, that is the action of a cut-on switch, can be obtained merely by subtracting the value of $y$ from 1 as represented by the right-hand vertical scale of sketch (a).

If the value of the base $e$ is changed, the value of the function at the operating point, where $x = 1$, can be changed. For instance, in the case of equation (2), changing the value of $e$ from its normal value of 2.7182 . . . to 10.0 produces the results indicated in sketch (b). Sketch (b) shows that

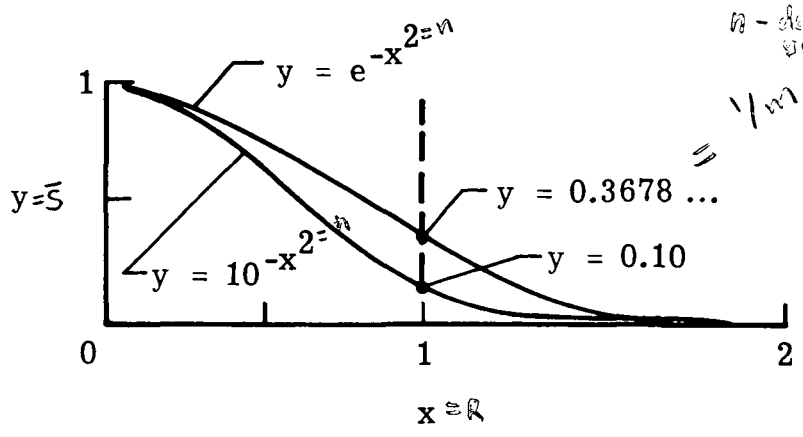


Sketch (b)

the new curve crosses at the operating point with a value of 0.10 and that the general shape of the two curves is essentially the same. In fact, the two curves are exactly the same if the scale of the X-axis for the new curve is changed as follows:

$$x_{10} = x_e\left(\sqrt{\frac{\ln e^{-1}}{\ln 10}}\right)^{1/2} = x_e\left(\sqrt{\ln 10}\right)^{1/2} \qquad (3)$$

Sketch (c) illustrates the comparisons after the scale changes are applied.

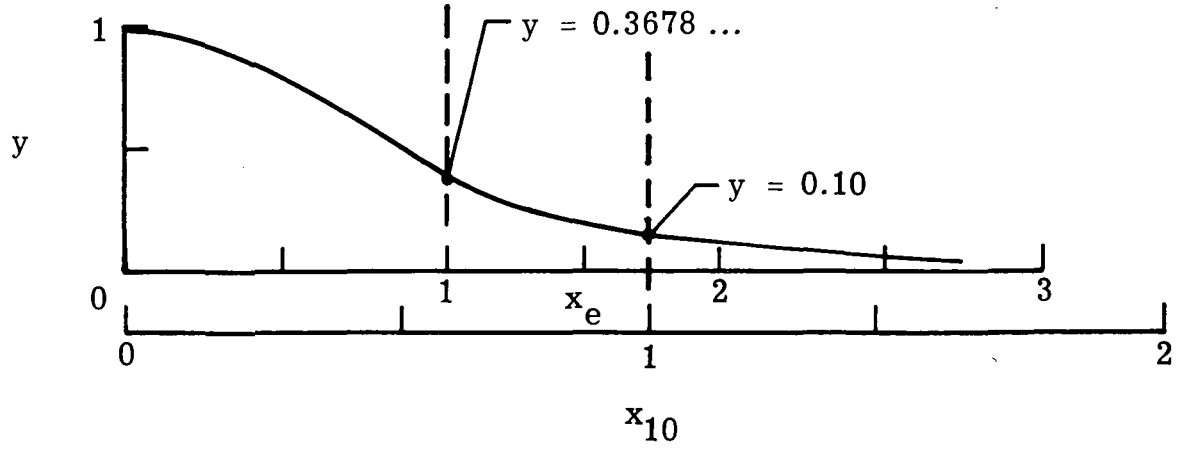


Sketch (c)

It is noted, therefore, that the only effect of changing the exponent-base value is to alter the position of the operating point along the curve. Thus, it is shown that the value of the exponent base and its related operating point can be treated in an arbitrary manner without influencing the basic shape of

the curve. That is to say, the gain and operating point for a given switching function can be treated as independent variables.

Based on these observations of the relationships exhibited by the two exponential equations (eqs. (1) and (2)), a generalized form of these equations was used to represent the desired cutoff function and is as follows:

$$\bar{S} = m^{-(R)^n} \tag{4}$$

where $\bar{S}$ represents the switching function which is on when $R = 0$ and switches to off as $R$ is increased, $n$ is any positive number used to define the switching gain or shape of the curve, $R$ is the nondimensionalized independent state variable, such as the ratio of $\alpha$ or $\beta$ to some reference value used to define the operating point for the function, and $m$ is the reciprocal of the decimal fraction of $\bar{S}$ at the operating point where $R = 1$.

The complement to $\bar{S}$ corresponding to a cut-on switch is represented by $\underline{S}$ and is related to $\bar{S}$ as follows:

$$\underline{S} = 1 - \bar{S} = 1 - m^{-(R)^n} \tag{5}$$

The position of the bar represents the value of the function when $R = 0$, that is, the bar above the $S$ denotes the on condition (value of 1) and the bar at the bottom denotes the off condition (value of 0).

The value of $m = 2$ was selected as a convenient base inasmuch as it corresponds to the operating point where $\bar{S} = \underline{S} = 0.5$. The characteristic shapes of the functions $\bar{S}$ and $\underline{S}$ for a value of $m = 2$ and several values of $n$ for the range of $R = 0$ to 1.6 are given in figure 1.

A system of subscripts is used to denote different switching functions applied to a given aerodynamic variable. For instance, in the case of the specific switching function that has its operating point located at some angle of attack with the value $\alpha_1$, the function is defined as

$$\bar{S}_{\alpha 1} = m^{-(R_{\alpha 1})^{n_{\alpha 1}}} \tag{6}$$

where $R_{\alpha 1} = \dfrac{\alpha}{\alpha_1}$, and $n_{\alpha 1}$ are the specific switching coefficients that define operating characteristics in the region of $\alpha = \alpha_1$. (Note that $m$ remains constant at the assigned value of 2 in all switching functions.)

The given form of the switching functions is convenient when used in a general equation. However, when used in a specific equation in which the values of the coefficients must be defined, the form is somewhat unwieldy, especially when more than one or two switching functions are involved. For example, the term $\bar{S}_{\alpha 1}$ might appear as $2^{-(\alpha/15.3^{o})^{4.6}}$. For convenience, a shortened form $\bar{S}_{\alpha}(15.3^{o},4.6)$ may be used. In this form, the specific values for the operating point and the gain factor are listed within the parentheses in the same sequence as they appear in the general form (eq. (6)) of the switching function. The numerical subscript is not necessary because it directly relates to the values within the parentheses and is therefore redundant.

The switching functions $\bar{S}$ and $\underline{S}$ can be applied both to a constant term, such as K, and to a variable term, such as K multiplied by $\alpha$, which involves the same variable as that which controls the switching function. In the case of the constant term, the complete term appears as $K\bar{S}_{\alpha}$ or $K\underline{S}_{\alpha}$, where the value of K is to be switched on or off as the value of $\alpha$ increases through the appropriate operating point (that is to say, where $R = 1$). The curves of figure 1(a), which is a plot of the variation of $\bar{S}$ and $\underline{S}$ with R for several values of n, can be used directly to visualize the curves represented by $K\bar{S}_{\alpha}$ and $K\underline{S}_{\alpha}$. The exact variation of these two terms can be obtained merely by multiplying the vertical-scale values of figure 1 by the value K and multiplying the horizontal-scale values by the value of $\alpha$ corresponding to the operating point. (Fig. 1(b) is a cross plot of fig. 1(a) for $R = 0.75$ and shows the effect of n on the values of $\bar{S}$ and $\underline{S}$ at these two specific points. Fig. 1(b) can be used as an aid in estimating the value of n required to produce a given curve shape.)

In the case of the variable term, the functions appear as $K\alpha\bar{S}_{\alpha}$ or $K\alpha\underline{S}_{\alpha}$. The purpose of the switching function is the same as for the previous case (constant term), which is to switch $K\alpha$ either off or on near some prescribed operating point. The curves of figure 2, which is a plot of the variation of $R\bar{S}$ and $R\underline{S}$ with R for several values of n, can be used to visualize the curves represented by $K\alpha\bar{S}_{\alpha}$ and $K\alpha\underline{S}_{\alpha}$.

## MODELING NONLINEAR LIFT CHARACTERISTICS

The subject modeling technique is a curve-fitting process in which a few relatively simple mathematical terms are coupled together by means of the previously discussed switching functions. In the case of the modeling lift coefficient, three terms are used. A reasonable fit is achieved by a trial-and-error process in which initial values for the various coefficients are selected by use of a semigraphical process and by reference to the curves of figures 1 and 2.

Several sources of information concerning lift characteristics at high angle of attack were reviewed to establish the trends in the static test data for several different general-aviation type configurations with unswept wings. The data covered models which varied from wing-alone models to complete models with different control deflections for values of angle of attack ranging from below $0^{\circ}$ up to $180^{\circ}$.

## Data Used for Analysis and Model Development

Reference 1 presents a general discussion of airfoil characteristics above the stall, in addition to supporting data derived from other sources such as reference 2. A portion of these data from reference 2 is presented in figure 3. This figure shows the two-dimensional airfoil lift data for the NACA 0012 airfoil section for the angle-of-attack range from $0^{\circ}$ to $90^{\circ}$ at a Reynolds number of $1.8 \times 10^{6}$.

A set of previously unpublished lift data for an approximately 1/6.5-scale model of a typical high-wing light airplane is given in figure 4 for the angle-of-attack range from $-4^{\circ}$ to $40^{\circ}$ for various combinations of the configuration components. These data were obtained in the Langley 12-foot low-speed tunnel at a Reynolds number of about $0.5 \times 10^{6}$.

The lift data presented in figure 5 were obtained from tests of a full-scale model of the same airplane used to obtain the data of figure 4. The tests (fig. 5) were conducted in the Langley full-scale tunnel and are reported in reference 3. These data for the configuration with the horizontal tail removed cover the angle-of-attack range from $-2^{\circ}$ to $24^{\circ}$ at a Reynolds number of about $2.8 \times 10^{6}$.

Lift data based on the results of tests of a 1/7-scale model of a low-wing light airplane reported in reference 4, are presented in figures 6 and 7. The tests were conducted in the Ames 12-foot tunnel for an angle-of-attack range from $-8^{\circ}$ to $90^{\circ}$ and covered several combinations of the configuration components (except wing alone) using three separate wings, all of the same planform but with different airfoil sections. These tests were made at two Reynolds numbers of $0.3 \times 10^{6}$ and $3.4 \times 10^{6}$. Additional component tests with one of the wings were made at intermediate Reynolds numbers of $0.6 \times 10^{6}$, $1.7 \times 10^{6}$, and $2.9 \times 10^{6}$. The lift curves for the model with the three wings and with the wings removed for the high Reynolds number condition are presented in figure 6, and the curves for the five different Reynolds number conditions with one of the wings are presented in figure 7.

All of the data presented are for the condition of no propeller and zero control deflections.

## Modeling Technique

Data analysis and model development.- In reviewing the data, it was observed that all of the data followed consistent trends throughout the angle-of-attack range and that the data in the stalled region, although somewhat more

erratic than for the unstalled region, were repeatable to a fairly reasonable degree. Furthermore, as illustrated in sketch (d),

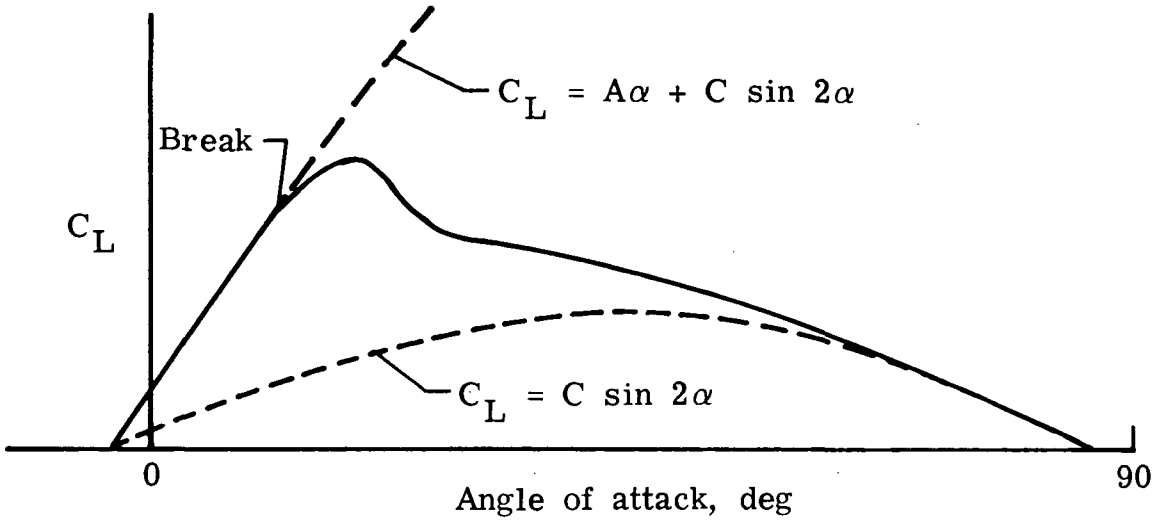


Sketch (d)

it was observed that the curve $C_L = C \sin 2\alpha$ (where $C$ is some constant value) provided a fairly close fit with the curves of figures 3, 6, and 7 for the angle-of-attack range above about 45°. The addition of a second term $A\alpha$ provided a very good fit at values of $\alpha$ below the break in the lift curve where flow separation does not occur.

The problem of obtaining a reasonable match for the angle-of-attack range above this breakpoint by using both the A-term and the C-term was partially solved by the development of the switching function $\bar{S}$. This function served the purpose of reducing the A-term to 0 as $\alpha$ increased beyond the breakpoint. The equation for the lift coefficient is now

$$C_L = A\alpha\bar{S}_{\alpha 1} + C \sin 2\alpha \tag{7}$$

Sketch (e) illustrates the promising results that were achieved after adjusting the values of $A$, $C$, $\alpha_1$, and $n_{\alpha 1}$ to obtain the desired fit. The contribution of $C_{L,A}$ and $C_{L,C}$, to the total lift coefficient $C_{L,A} + C_{L,C}$ is indicated by the two dashed curves. After obtaining a reasonable match for each of several sets of the test data, it was observed that in all cases there was a region, indicated by the cross-hatched area of sketch (e), where the equation was consistently deficient; this region extended from about $C_{L,max}$ to an angle of attack of about 60°. So as to overcome this problem, a third term was added to equation (6) as follows:

$$C_L = A\alpha\bar{S}_{\alpha 1} + B\underline{S}_{\alpha 2}\bar{S}_{\alpha 3} + C \sin 2\alpha \tag{8}$$

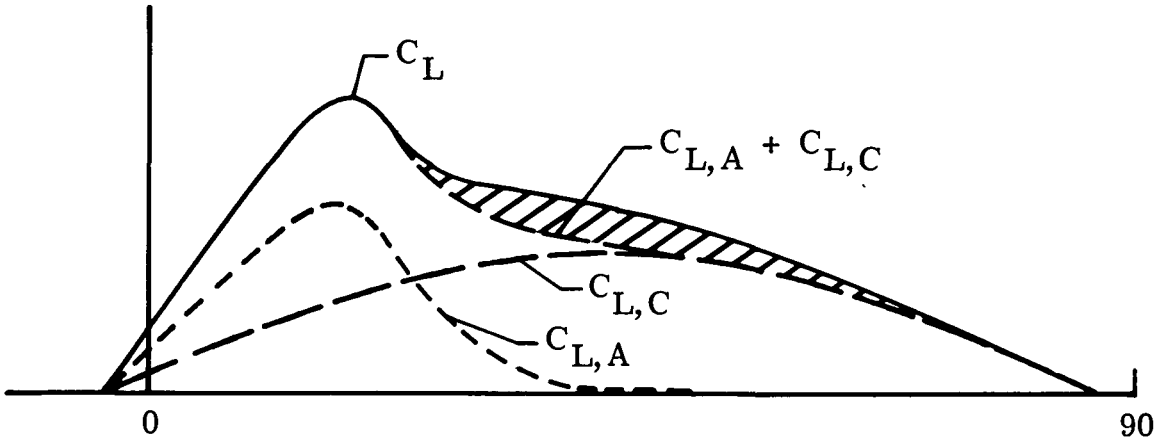


Sketch (e)

The coefficients for equation (7) and those for the new B-term of equation (8) were adjusted to produce results such as those illustrated in figure 8. This figure presents the wing-alone data from figure 4. The calculated values matched the measured values of the force test data generally to within about 2 to 4 percent of $C_{L,max}$ which is estimated to be as good as or better than the accuracy or repeatability of the original measured data. Also shown in figure 8 are the contributions of each of the three terms (eq. (8)) to the lift coefficient. It can be observed that $\underline{S}_{\alpha 2}$ causes the contribution of the B-term to increase with $\alpha$ at about the same time that the contribution of the A-term decreases. These trends are due to the fact that the values of $\alpha_1$ and $\alpha_2$ (fig. 8 and table I) are close. Furthermore, $\bar{S}_{\alpha 3}$ causes the contribution of the B-term to reduce gradually to 0 as the angle of attack increases to some point beyond $40^o$.

As an initial check on the applicability of equation (8) to a variety of other test conditions and configurations, the data for the full-scale model, as presented in figure 5, were employed. The wing-alone lift curve shown in figure 9 was obtained by subtracting the fuselage-alone data of figure 4 from the wing-fuselage data of figure 5 because the full-scale data were not obtained for these conditions and it was believed that the differences due to Reynolds number were small. The coefficients of equation (8) were adjusted, and the resulting calculated lift variations, obtained after several iterations, are also presented in figure 9. Because the data were limited to an angle of attack of $24^o$, a few degrees past that for $C_{L,max}$, it could not be determined that the equation (eq. (8)) was suitable for the range of angle of attack above this point; however, for the range covered by the data points, the match is considered to be very good.

As a further check on the applicability of equation (8), particularly for the higher angles of attack, the coefficients were readjusted to obtain the lift curves for the wings of the low-wing model with three different airfoils and with a planform different from that of the high-wing model. The results are illustrated in figure 10, which also presents the estimated wing-alone lift

based on the data of figure 6. The estimated lift data for the wing-alone configuration, which was not tested, were obtained by subtracting the test data for the fuselage and horizontal-tail configuration from those for the complete model configurations. The wing-off data for $N_{Re} = 3.4 \times 10^6$ were used in obtaining the wing-alone lift curves because tests were not run at intermediate Reynolds numbers. Furthermore, although not presented here, comparison of the data from reference 4 for low and high Reynolds numbers showed negligible effect of Reynolds number on the lift of the fuselage and horizontal-tail configuration. The match between the calculated lift values (using eq. (8)) and the estimated wing-alone data of figure 10 is seen to be as good as that presented in figures 8 and 9. It is interesting to note that, by suitable adjustment of the switching coefficients, the curves for the calculated values have been made to follow the rather unusual appearing undulations in the region of maximum lift. No attempt was made to match the relatively small lift variation near an angle of attack of $90^\circ$ which is considered to be of no significance for normal problems. If it were considered to be essential, an additional term similar to the B-term with appropriate coefficients could have sufficed to achieve a good match in that part of the curve.

The final check on the applicability of equation (8) was made by attempting to match the set of wing-alone lift curves which were determined for one of the three previous wings in tests conducted at four lower Reynolds number conditions. The wing-alone data points were estimated by using the data given in figures 6 and 7. The resulting match for each condition, as illustrated in figure 11, was similar to that for the previous cases.

For reference, the values of the coefficients for all of the wings and their test conditions are listed in table I, along with the values of the appropriate geometric characteristics of the four different wings. The variations with Reynolds number of the coefficient values for some of these wings are shown in figure 12, in which the values are plotted against Reynolds number. For clarification, the symbols for each coefficient have been joined by straight lines. This figure (fig. 12) shows generally uniform and consistent trends with Reynolds number.

Significance of individual terms.- The lift mathematical model, given by equation (8), was developed strictly on an intuitive and empirical basis with the curve-fitting technique employing relatively simple mathematical terms. At this point in time, no theoretical analysis has been developed to support the formulation of these terms; however, the apparent high degree of correlation over the very large angle-of-attack range suggests that some physical significance can be attached to the individual terms.

In general, it appears that the A-term relates primarily to the vortex or circulation about the airfoil for the unseparated flow conditions, that the B-term relates to a more complex vortex system after flow separation has occurred, and that the C-term relates to the lift generated by impact pressures acting directly on the lower surface throughout the whole angle-of-attack range. Although there is no rigorous proof of these relationships, these apparent relationships should be helpful in understanding and visualizing the contributions of each of the elements.

Initial approximations.- Analysis of the original data curve to obtain the initial approximations for the coefficients is accomplished with the aid of a few key points on the lift curve. Sketches (f) and (g) illustrate two basic types of lift curves that have been evaluated and identifies these key points for each curve.

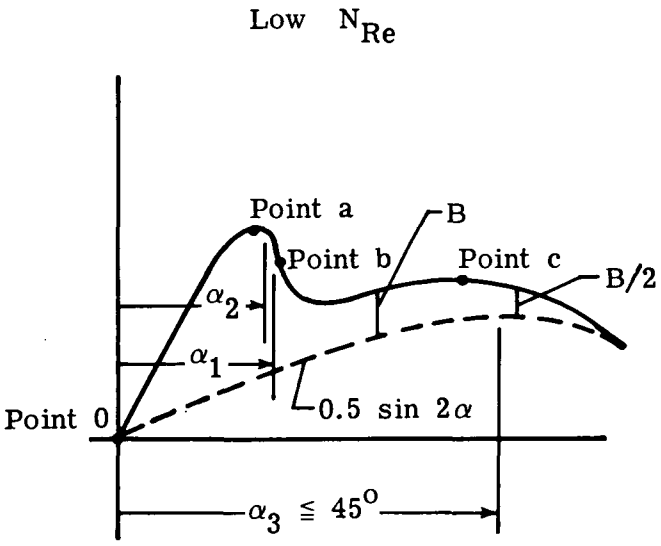


Sketch (f)

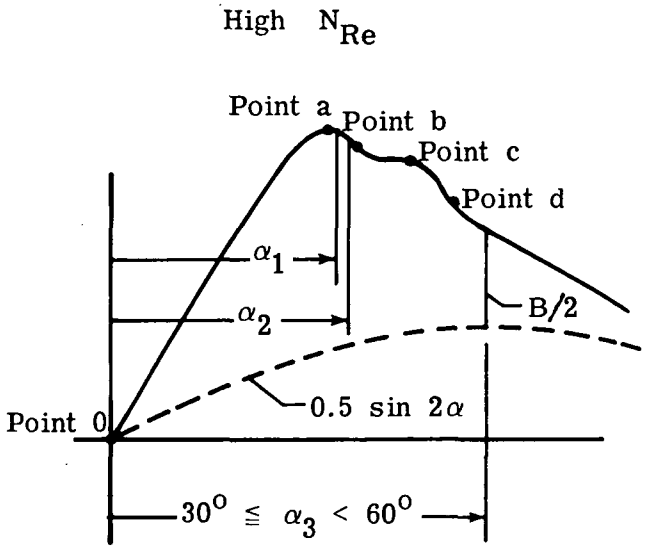


Sketch (g)

Sketch (f) represents a typical lift curve for a wing obtained at relatively low Reynolds numbers generally on the order of about $0.6 \times 10^6$ or less, and sketch (g) represents that obtained at high Reynolds numbers. The key points are identified as points 0, a, b, c, and d. The first key point, point 0, corresponds to the angle of attack where $C_L = 0$, and points a and c correspond to first and second peaks on the lift curve. The key point b represents the point of maximum negative lift-curve slope between points a and c, whereas point d is a similar point for the high Reynolds number data that is not always very well defined but is evident in some data a few degrees above point c.

## Determination of Values for Coefficients

Early in the process of developing equation (8), it was observed that the three-dimensional-flow lift characteristics of all the wings, regardless of aspect ratio, planform, and Reynolds number, were quite similar for angles of attack above about $45^o$. In reference 2, which presents the two-dimensional-flow data included as figure 3 in the present report, a similar effect is also noted and is observed to extend to angles of attack up to about $135^o$. For this latter case of two-dimensional-flow data, however, the lift appears to be about twice that for the three-dimensional-flow data. Inasmuch as the A-term and B-term of equation (8) are effectively switched off by the functions $\bar{S}_{\alpha 1}$ and $\underline{S}_{\alpha 2}$ for this high angle-of-attack region, the C-term accounts for essentially all the lift in the fully stalled condition. The implication of this point,

at least for three-dimensional-flow conditions, is that the C-coefficient is therefore constant for all wing configurations and test conditions. The results of the curve-fitting process as presented in table I did, in fact, show that the value of the C-coefficient could have a constant value of 0.5. Consequently, at least until more complete and detailed data indicating otherwise are obtained, it is assumed that this value is applicable to all three-dimensional wings regardless of their geometric characteristics or operating Reynolds number.

Although the two-dimensional-flow lift characteristics are not modeled in this study, it appears evident that the value of C for this flow condition is likely to be somewhat larger than 0.5.

For the small angles of attack where $\bar{S}_{\alpha 1} \approx 1$, $\underline{S}_{\alpha 2} \approx 0$, and $\sin 2\alpha \approx 2\alpha$, equation (8) reduces to

$$C_L = A\alpha + C2\alpha \tag{9}$$

By rearranging terms and substituting the assumed value for C of 0.5, the value of A is shown to be uniquely determined as follows:

For $\alpha$ in radians,

$$A = C_{L_\alpha} - 1 \qquad /RAD \tag{10a}$$

For $\alpha$ in degrees,

$$A = C_{L_\alpha} - 0.0175 \qquad /DEG \tag{10b}$$

where $C_{L_\alpha}$ is the usual wing-alone lift-curve slope for the linear portion of the lift curve at low angles of attack.

No suitable method for directly determining the values for the remaining coefficients has been developed. Consequently, it has been necessary to resort to an iterative process to derive the desired values. This process consists of two parts. In the first, initial approximations are obtained by qualitative analysis of the data curve; in the second, which is the curve-fitting process, these inital values are inserted in the lift equation (8) and a plot of the calculated lift coefficients is compared with the original data plot over the angle-of-attack range covered by those data. On the basis of the differences between the two plots, the values are altered until a reasonable match is obtained. Familiarity with this iterative process greatly facilitates use of the technique because of its reliance on human judgment to obtain an acceptable result with a minimum of effort. The following discussion covers a few guidelines for carrying out the two separate steps.

The guidelines for estimating the values of the coefficients based on a qualitative analysis of the complete series of data curves covered in this report are summarized as follows (see sketches (f) and (g)):

(1) The value of $\alpha_1$ generally corresponds to the angle-of-attack increment between point 0 and a point falling between point a and point b.

(2) The value of $\alpha_2$ is generally within $\pm 2^\circ$ of that for $\alpha_1$. At lower Reynolds numbers, $\alpha_2$ tends to be less than $\alpha_1$, and vice versa.

(3) The value of $\alpha_3$ generally corresponds to a point located between $30^\circ$ and $60^\circ$ above point 0. For low Reynolds numbers, this point falls a few degrees beyond point c. For higher Reynolds numbers, this point tends to fall above point d.

(4) The value of B can be estimated on the basis of the difference at $\alpha_3$ between the data curve and the curve (dashed) corresponding to the C-term; that is, $C_{L,C} = 0.5 \sin 2\alpha$. This difference is approximately equal to B/2. The value of B generally increases with Reynolds number.

(5) For certain low Reynolds numbers, some portion of the curve between point b and point c may be parallel, or nearly so, to the curve corresponding to the C-term. In such cases, the difference between the two curves in that portion corresponds to the value of B, and the value of $\alpha_3$ corresponds to the point along the curves where the difference is equal to B/2.

(6) Larger values of n correspond to sharper changes in the lift curve. (See figs. 1 and 2.) Values of $n_{\alpha 1}$ tend to fall in the range of 5 to 10; those for $n_{\alpha 2}$, in the range of 8 to 16; and those for $n_{\alpha 3}$, in the range of 3 to 7. These tendencies can be observed in figure 12.

## Curve Fitting

The curve-fitting process is initiated by inserting the approximated values into equation (8) and plotting the resulting lift values on a copy of the original lift-data plot. It is preferable, where possible, to use the same angle-of-attack values as the original lift data so that comparisons can be made directly on a point-to-point basis. However, a faired curve should be drawn through both sets of lift points to facilitate the fitting process.

A basic step to the fitting process is to observe the match that is obtained in the various sections of the curves. These sections are indicated in sketch (h). Section I corresponds to that linear portion of the lift curve below the stall, with its upper limit located at about one-half the value of $\alpha_1$. Section II extends from this point to a point about halfway between the points corresponding to $\alpha_1$ and $\alpha_3$ and is divided in two parts of $\alpha_1$. Section III extends from this point to about $60^\circ$ angle of attack where the total lift curve tends to match that for the C-term. From this point on, in section IV, the two curves should match very closely regardless of the values

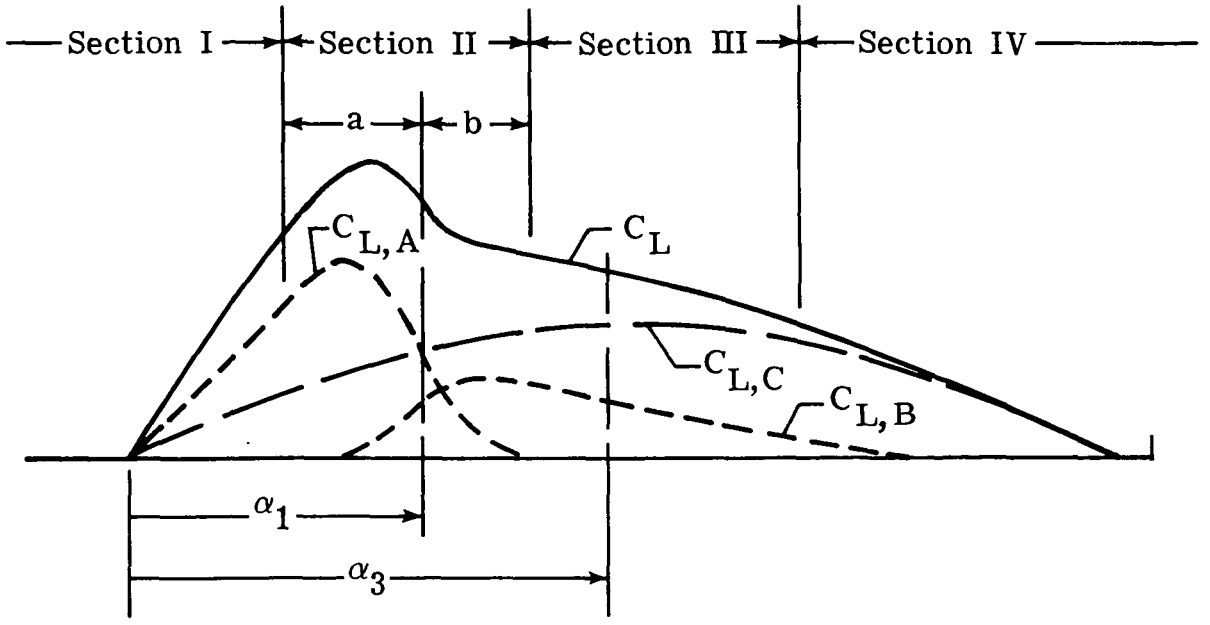


Sketch (h)

in the A-term and the B-term. The following tabulation lists those factors of equation (8) that, in addition to the C-term, have a primary effect in each of the designated sections of the curve:

| Section | Factors of equation (8) |
|---|---|
| I | A |
| IIa | A, B, $\bar{S}_{\alpha 1}$, and $\underline{S}_{\alpha 2}$ |
| IIb | B, $\underline{S}_{\alpha 2}$, and $\bar{S}_{\alpha 3}$ |
| III | B and $\bar{S}_{\alpha 3}$ |
| IV | --- |

It is doubtful that there will be any difficulty in obtaining a satisfactory match for section I because this section is strictly a function of the portion of the original data curve which is usually linear. However, if there is any mismatch it must be corrected before attempting to correct the rest of the curve. In section IIa, mismatch is primarily a function of A, B, $\bar{S}_{\alpha 1}$, and $\underline{S}_{\alpha 2}$. In this region, $\bar{S}_{\alpha 3}$ is essentially switched fully on and has no significant influence. Mismatch in the next portion, section IIb, is a function of the values for B, $\underline{S}_{\alpha 2}$, and $\bar{S}_{\alpha 3}$ inasmuch as $\bar{S}_{\alpha 1}$ is essentially switched fully off. In section III, $\underline{S}_{\alpha 2}$ is essentially switched fully on and $\bar{S}_{\alpha 3}$ gradually switches off, leaving only the C-term in the last portion (section IV).

The most difficult sections in which to obtain a reasonable match are obviously sections IIa and IIb where the airflow is in a state of partial separation and the number of variables involved is the greatest. Consequently,

attention should be directed here following that given in section I. By using this sequence, the values for B and $\alpha_1$ are usually sufficiently well defined so that only the switching coefficients for $\bar{S}_{\alpha 3}$ need be adjusted to obtain a reasonable fit in the remaining portions.

An aid, in the form of a set of lift curves based on an arbitrary set of coefficient values, is presented in figure 13 to assist in the process of adjusting the values of the variable coefficients to achieve the desired fit at the different parts of the curve. These curves provide the user with a qualitative visual indication of the sensitivity of the curve shape to changes in the factors of equation (8). The value of each of the coefficients, except for the n-coefficients, was changed by ±10 percent of the nominal value. The coefficients $n_\alpha$ were changed by ±30 percent so as to show recognizable changes. The influences or effects of the various coefficients in the different sections of the curve are consistent with the listing of terms given in the preceding tabulation.

Although the shape of the basic curve can be altered significantly by using other sets of nominal values, it is believed that the incremental trends noted herein will not be significantly different. Consequently, it is believed that these curves should be helpful to the user even though the shape of the curve in question is considerably different.

The term "reasonable fit or match" has been used at various points in this discussion without a definition of a criterion for judging the adequacy of the results. For the most part, the user must establish his own criterion based on the use to which the mathematical model is to be applied and on the angle-of-attack range in question. He should bear in mind that the data at the stall, and beyond, tend to be more erratic and less repeatable than for lower angles of attack. Consequently, a "reasonable fit" in the high angle-of-attack region very likely will have more discrepancies between the model and the data points than for the lower angle-of-attack region. It is likely that the region beyond both parts of section II can be ignored for most applications. For the present purposes, however, showing that a match could be obtained within about 4 percent of the maximum lift coefficient for any angle of attack within the range of about $0^\circ$ to $90^\circ$ was considered to be a reasonable goal.

The curves of figure 1(a), which show the variations of $\bar{S}$ and $\underline{S}$ with R for different values of n, reveal that there can be significant ranges of R-values for which $\bar{S}$ or $\underline{S}$ have essentially the value of either 1 or 0. The ranges of R-values are dependent on the value of n. If the user is interested in simplifying the curve-fitting process and reducing computational effort by accepting a small and well-defined error in the calculated lift terms, the switching functions can be preset to either 1 or 0 for calculations in which the value of R falls within these particular ranges. These ranges are illustrated in figure 14 which is a plot of combinations of R and n for which $\bar{S}$ and $\underline{S}$ have the values of 0.99, 0.98, and 0.96 or 0.01, 0.02, and 0.04. The resulting curves represent the boundary combinations of R- and n-values for errors of 1, 2, and 4 percent, assuming values of $\bar{S}$ and $\underline{S}$ equal to 1 or 2. For combinations falling in the regions external to the two groups of curves, the functions can be either 1 or 0, depending on the desired accuracy. For

other values in the region between the two groups of curves, the complete calculations of $\bar{S}$ or $\underline{S}$ and related terms should be performed.

## Influences of Wing Geometry and Operating Conditions on Coefficients

At this point, only limited information is available on the influences of the geometric characteristics of the wing and of the operating conditions of the airstream on the coefficients of the lift mathematical model. Consequently, equation (8) cannot be used as a predictive tool to calculate the lift characteristics of a wing of completely arbitrary geometric characteristics. However, it is possible that continued use as an empirical tool will help to establish the effects of various geometric characteristics.

As previously noted, a constant value of 0.5 for the C-coefficient was found to produce desirable matches for all of the three-dimensional flow data analyzed in this study. Consequently, it is tentatively concluded that this term is independent of geometric or Reynolds number effects. However, this should not be treated as a firm conclusion until a much greater supply of test data has been analyzed for a large variety of wings and test conditions.

Equations (10) indicate that the A-coefficient is a direct function of the lift-curve slope $C_{L_\alpha}$ of the wing. It is concluded, therefore, that the value of this coefficient will vary in the same manner as $C_{L_\alpha}$ with changes in wing planform factors such as aspect ratio, taper ratio, and sweepback. Furthermore, the coefficient should be essentially independent of the influences of airfoil section characteristics and Reynolds number, as is the case of $C_{L_\alpha}$ for unseparated flow conditions.

The remaining coefficients appear to relate to the buildup of separated flow conditions and, consequently, should be influenced by those factors that are known to influence the separation phenomenon. It is important to note that these terms relate to the wing as a whole and represent not only the separation characteristics of the basic airfoil section of the wing but also the propagation of the separation along the span of the wing. The partial list of factors influencing the initiation and propagation of separation is as follows: airfoil section, surface roughness or features, Reynolds number, spanwise twist, aspect ratio, taper ratio, sweepback, Mach number, fuselage interference, control-surface deflections, and propeller slipstream effects.

Some indication of the influence of Reynolds number and airfoil section on various terms can be observed in table I, which lists the values of the terms for the wings of two different planforms and for the one wing tested with three different airfoil sections and at different Reynolds numbers. The values obtained from this table and plotted in figure 12 reveal a somewhat systematic variation with Reynolds number. However, no conclusions can be drawn from these specific results.

## OTHER APPLICATIONS OF MODELING TECHNIQUE

Although this paper has been specifically directed toward the mathematical modeling of the lift characteristics of straight wings, there are many other applications, both aerodynamic and nonaerodynamic, to which this technique can be directed. In fact, the technique has been used in defining a complete set of aerodynamic characteristics of a particular complete airplane configuration for use in a simulation study of the stall and spinning dynamics of the configuration. The mathematical models were based on a set of static force test data covering large angle-of-attack and sideslip ranges and were used to calculate a set of related rotary characteristics which were not measured. The mathematical models were developed for each of the major components of the airplane: wing, fuselage, and tail members. A sample of these models is briefly discussed to illustrate how the switching functions have been applied to another type of aerodynamic term.

### Drag of Wing-Fuselage Combination

The mathematical model for drag of the wing-fuselage combination was developed by using the classical equation for the profile and induced drag as the base equation. Additional terms were added to account for the mismatch that resulted at the higher angles of attack. The result is as follows:

$$C_D = \left[D + E(C_{L,w})^2\right] \bar{S}_{\alpha 4} + (F \cos^2 \alpha + G \sin^2 \alpha) \underline{S}_{\alpha 4} \qquad (11)$$

The D- and E-terms that represent the classical drag equation were switched off by $\bar{S}_{\alpha 4}$ because they did not appear to be appropriate for conditions where vortex lift was becoming small and separated flow wake was very large. The new terms were added to account for these high drag conditions of separated flow and were switched on by the complement of $\bar{S}_{\alpha 4}$. The match of the calculated values with the extracted test data is shown in figure 15.

### Nonaerodynamic Applications

In view of the high degree of flexibility in adjusting the switching-function characteristics, there appear to be numerous applications for these functions in other fields where nonlinear phenomena are encountered. A few examples that illustrate the scope of possible applications are as follows:

(1) Saturation effects in magnetics and electronics.

(2) Hydraulic and pneumatic valve design.

(3) Structural loading beyond the elastic limits of materials.

## CONCLUDING REMARKS

A mathematical-modeling technique has been developed for the lift characteristics of straight wings throughout a very wide angle-of-attack range. The technique employs a mathematical switching function that facilitates the representation of the nonlinear aerodynamic characteristics in the partially and fully stalled regions and permits matching empirical data within ±4 percent of maximum values. Although specifically developed for use in modeling the lift characteristics, the technique appears to have other applications in both aerodynamic and nonaerodynamic fields.

Langley Research Center
National Aeronautics and Space Administration
Hampton, VA 23665
July 26, 1978

## REFERENCES

1. Hoerner, Sighard F.; and Borst, Henry V.: Fluid-Dynamic Lift. Hoerner Fluid Dynamics, Brick Town, N.J., c.1975.

2. Critzos, Chris C.; Heyson, Harry H.; and Boswinkle, Robert W., Jr.: Aerodynamic Characteristics of NACA 0012 Airfoil Section at Angles of Attack From 0° to 180°. NACA TN 3361, 1955.

3. Greer, H. Douglas; Shivers, James P.; and Fink, Marvin P.: Wind-Tunnel Investigation of Static Longitudinal and Lateral Characteristics of a Full-Scale Mockup of a Light Single-Engine High-Wing Airplane. NASA TN D-7149, 1973.

4. Bihrle, William, Jr.; Barnhart, Billy; and Pantason, Paul: Static Aerodynamic Characteristics of a Typical Single-Engine Low-Wing General Aviation Design for an Angle-of-Attack Range of -8° to 90°. NASA CR-2971, 1978.

TABLE I.- MATHEMATICAL-MODEL COEFFICIENTS FOR NONLINEAR LIFT CHARACTERISTICS OF SEVERAL WINGS[a]

| Airfoil | Planform | $N_{Re}$ | Reference | $\alpha_o$, deg | A, per deg | $\alpha_1$, deg | $n_1$ | B | $\alpha_2$, deg | $n_2$ | $\alpha_3$, deg | $n_3$ | C |
|---|---|---|---|---|---|---|---|---|---|---|---|---|---|
| High-wing model | | | | | | | | | | | | | |
| NACA $64_2A215$ and NACA $64_1A412$ | Aspect ratio of 7.7; semitapered | $0.5 \times 10^6$ | Present paper | [b]-4.4 | 0.064 | 15.8 | 5 | 0.30 | 14.4 | 7.5 | 60 | 7.0 | 0.5 |
| | | $2.6 \times 10^6$ | 3 | [b]-2.3 | .060 | 22.5 | 7.5 | .63 | 22.0 | 10 | 37 | 3.0 | .5 |
| Low-wing model | | | | | | | | | | | | | |
| NASA $64_2$-415 | Aspect ratio of 6.1; constant chord | $0.3 \times 10^6$ | 4 | -6.1 | 0.051 | 16.5 | 7.0 | 0.17 | 15.0 | 13 | 50 | 7.0 | 0.5 |
| | | .6 | 4 | -6.1 | .051 | 17.6 | 6.5 | .17 | 15.9 | 16 | 50 | 7.0 | .5 |
| | | 1.7 | 4 | -6.1 | .051 | 22.7 | 5.0 | .27 | 24.2 | 14 | 45 | 3.0 | .5 |
| | | 2.9 | 4 | -6.1 | .051 | 23.0 | 7.8 | .56 | 24.0 | 15 | 37 | 3.0 | .5 |
| | | 3.4 | 4 | -6.1 | .051 | 23.0 | 8.0 | .56 | 23.7 | 14 | 37 | 3.0 | .5 |
| NACA $64_2$-415 (drooped L.E.) | | $3.4 \times 10^6$ | 4 | -8.0 | 0.051 | 26.2 | 0.5 | 0.90 | 27.2 | 16 | 39 | 2.5 | 0.5 |
| NASA GAW-1 | | $3.4 \times 10^6$ | 4 | -5.8 | 0.051 | 26.2 | 0.5 | 0.95 | 27.2 | 16 | 40 | 2.5 | 0.5 |

[a]Coefficients are for measured or estimated wing-alone data. Where specific wing-alone were not available, estimates were obtained by subraction of measured or estimated component contributions.

[b]Difference due to different reference axes.

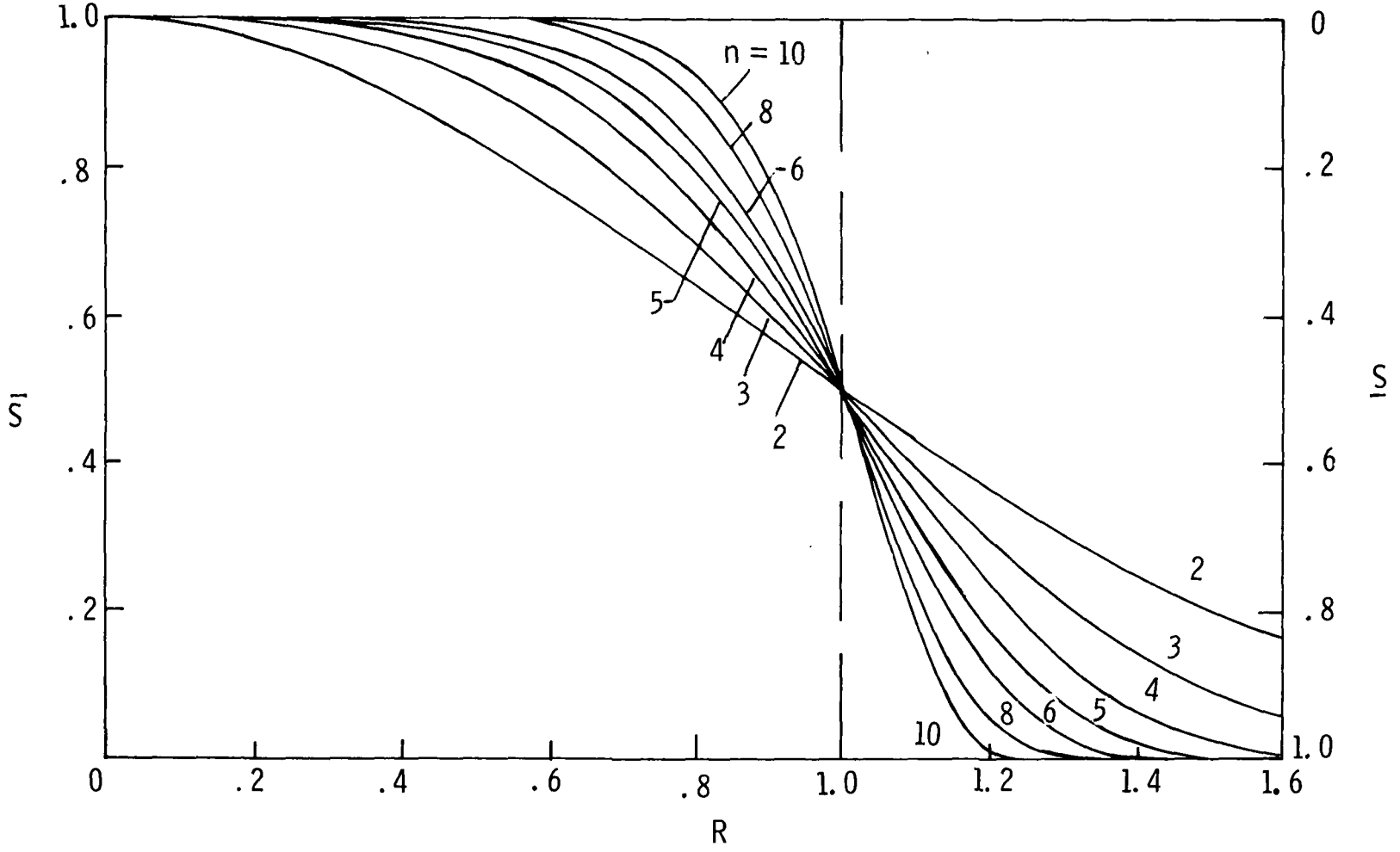


(a) Variation of $\bar{S}$ and $\underline{S}$ with R for several values of n.

Figure 1.- Variation of R and n with switching functions $\bar{S} = m^{-(R)^n}$ and $\underline{S} = 1 - \bar{S}$ for m = 2.

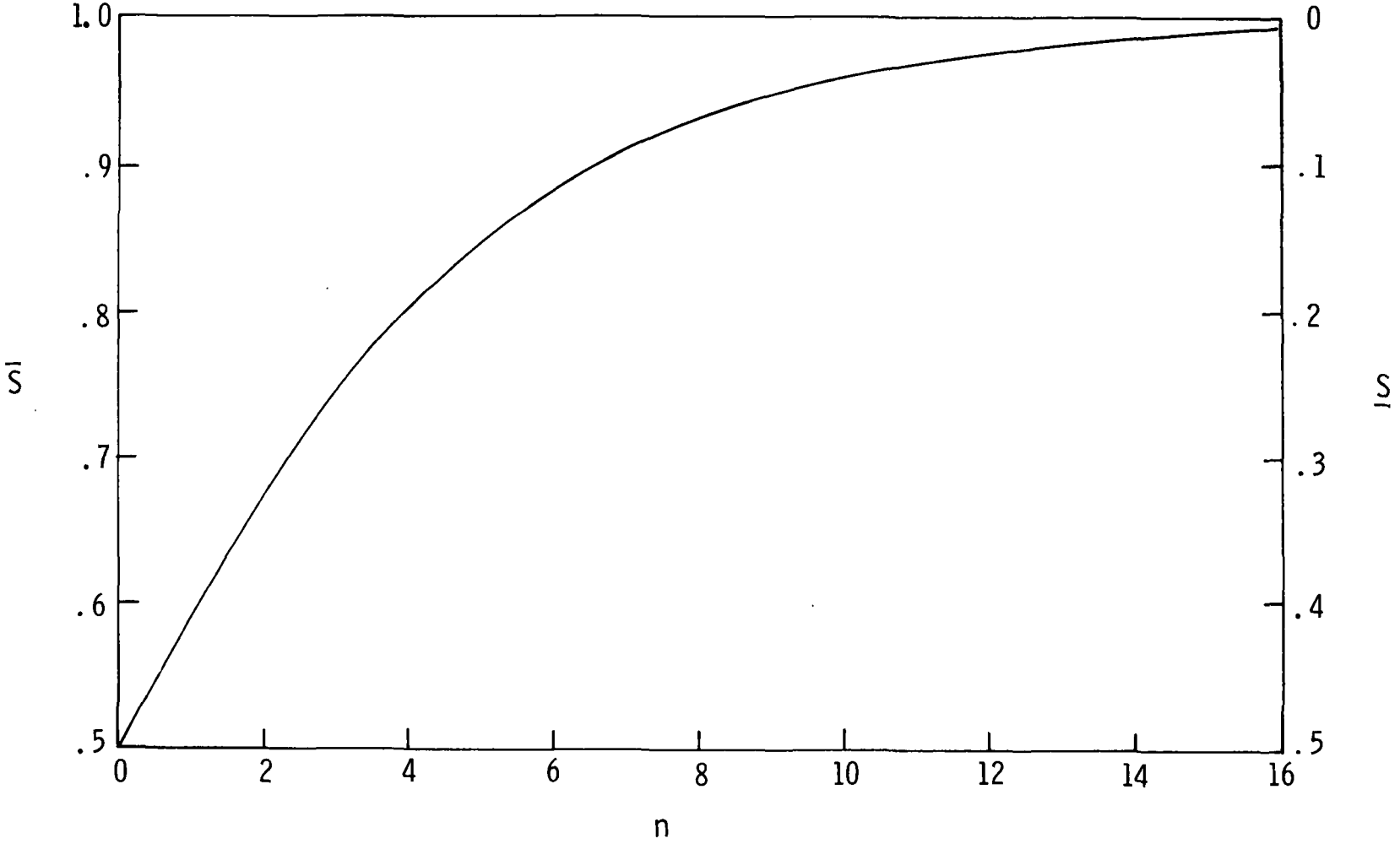


(b) Variation of $\bar{S}$ and $\underline{S}$ with n for R = 0.75.

Figure 1.- Concluded.

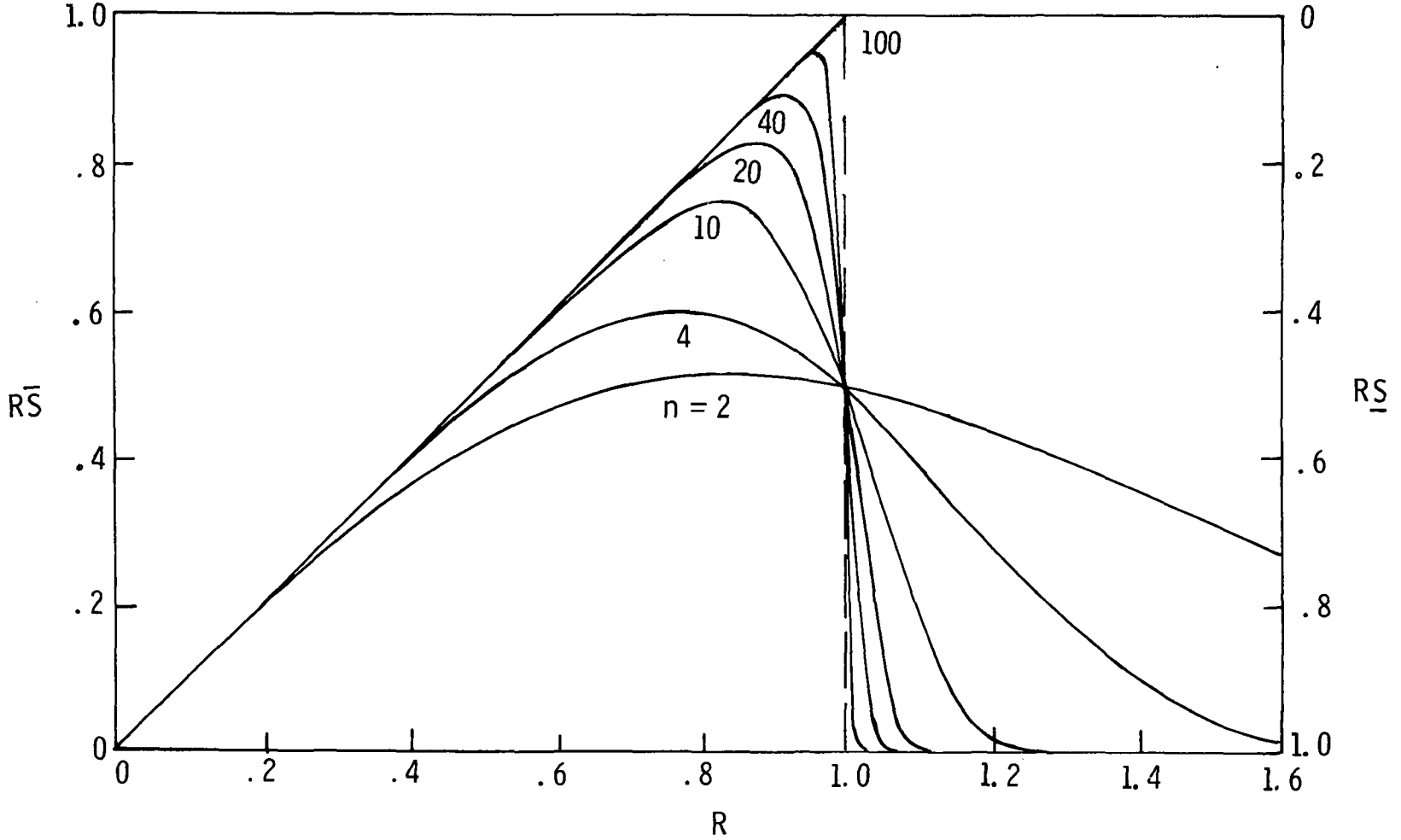


Figure 2.- Variation of R with switching functions $R\bar{S} = m^{-(R)^n}$ and $R\underline{S} = 1 - R\bar{S}$ for several values of n and for m = 2.

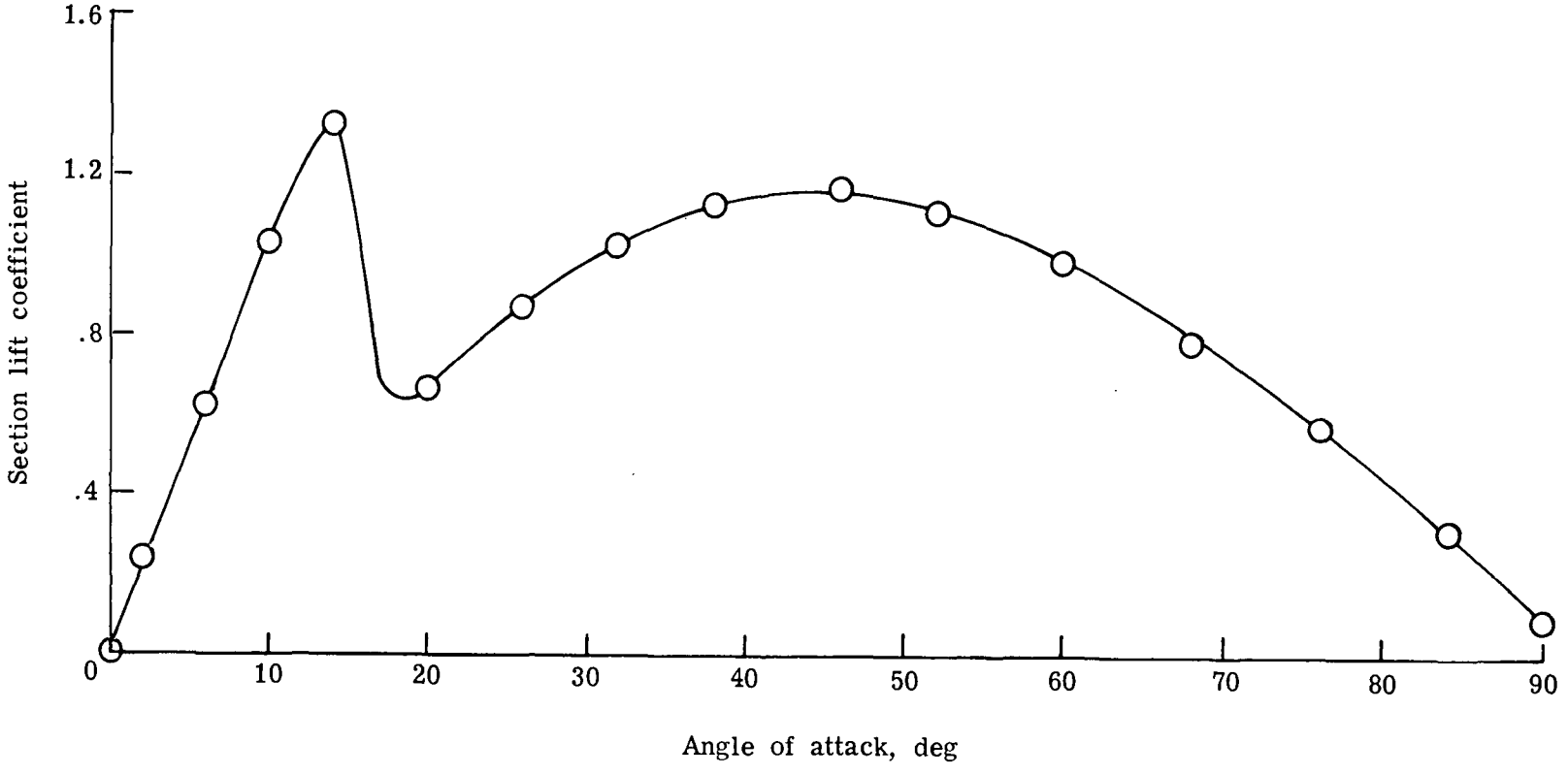


Figure 3.- Variation of NACA 0012 section lift coefficient with angles of attack from $0^{o}$ to $90^{o}$ at $N_{Re} = 1.8 \times 10^{6}$. Data obtained from reference 2.

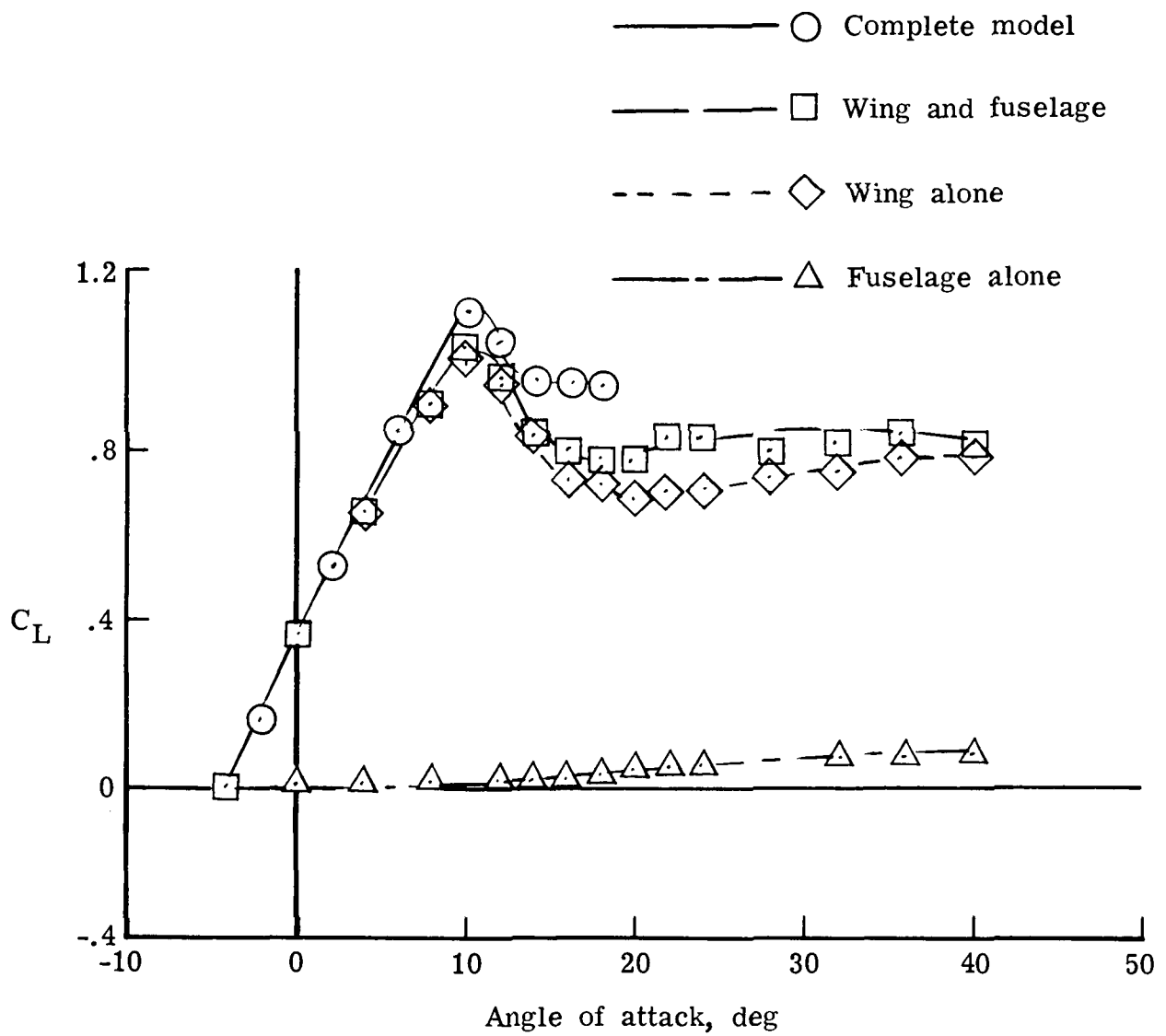


Figure 4.- Variation of lift coefficient with angle of attack from -4° to 40° for approximately 1/6.5-scale model of typical high-wing light airplane with various components at $N_{Re} \approx 0.5 \times 10^6$. Data obtained from unpublished tests in Langley 12-foot low-speed tunnel.

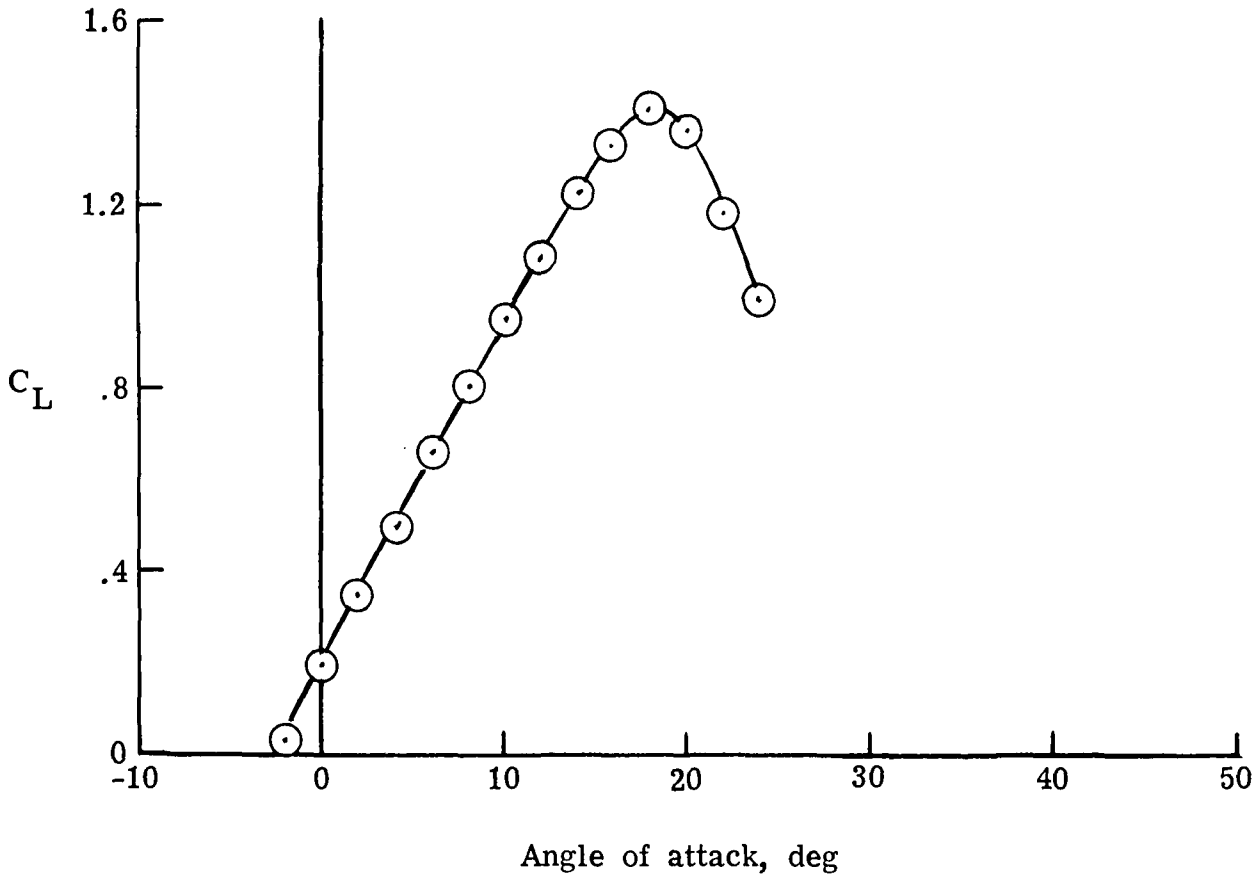


Figure 5.- Variation of lift coefficient with angle of attack from -2° to 24° for full-scale model of typical high-wing light airplane with horizontal tail removed at $N_{Re} \approx 2.8 \times 10^6$. Data obtained from reference 3.

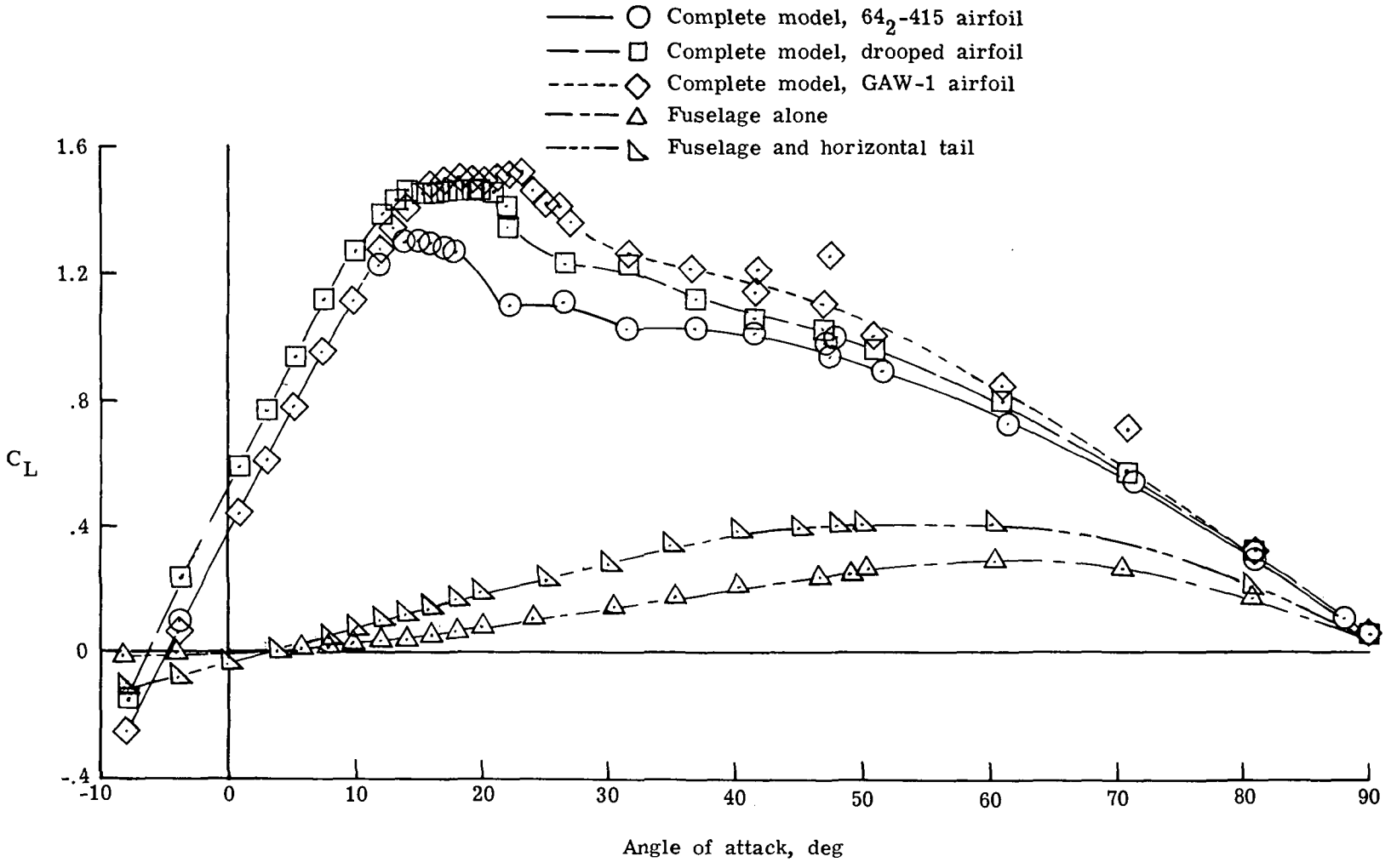


Figure 6.- Variation of lift coefficient with angle of attack from -8° to 90° for complete 1/7-scale model of typical low-wing light airplane with various components, including three separate wings with different airfoil sections at $N_{Re} = 3.4 \times 10^6$.

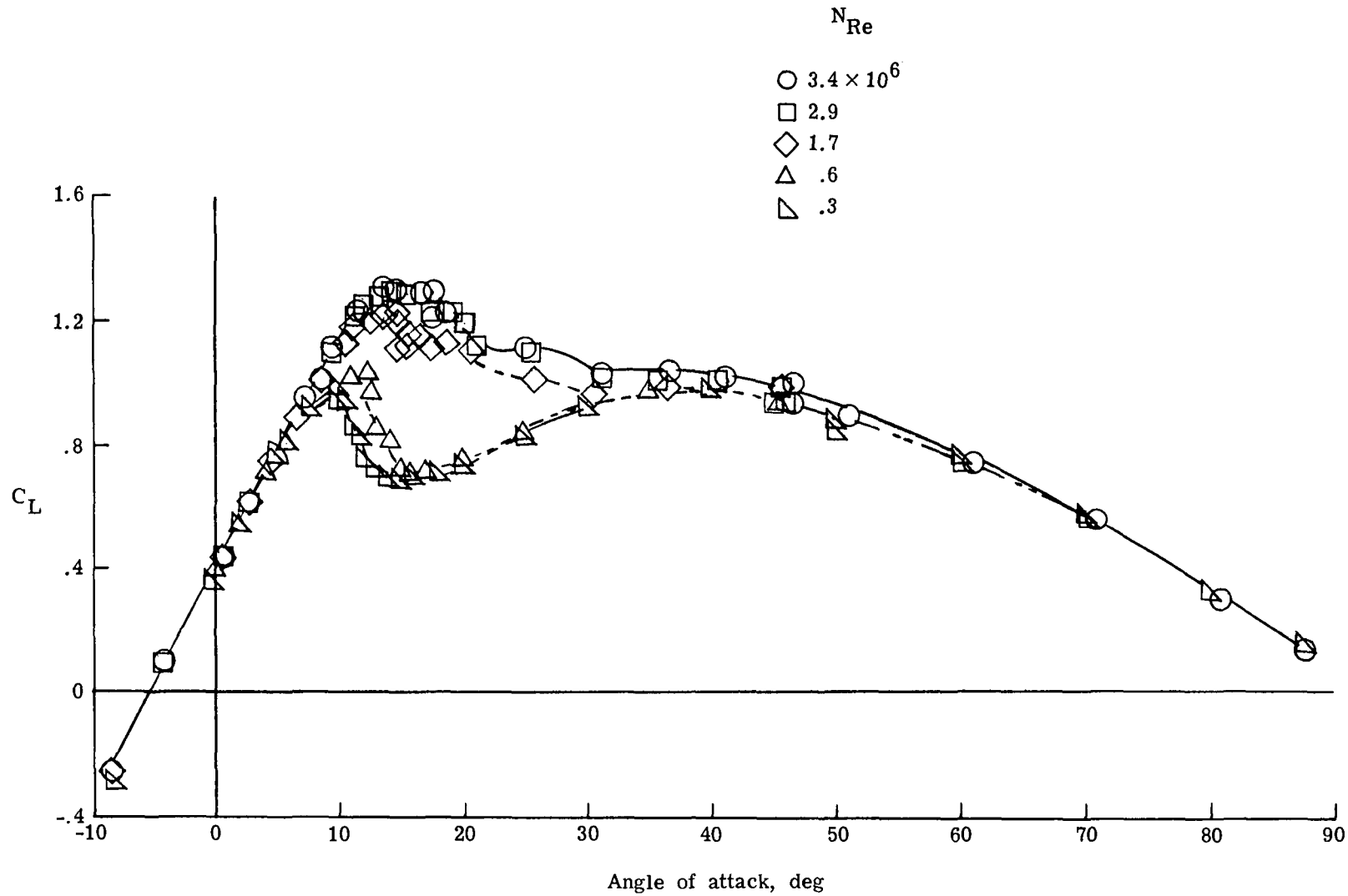


Figure 7.- Variation of lift coefficient with angle of attack from -8° to 90° for 1/7-scale model of typical low-wing light airplane with NACA $64_2$-415 airfoil at several Reynolds numbers.

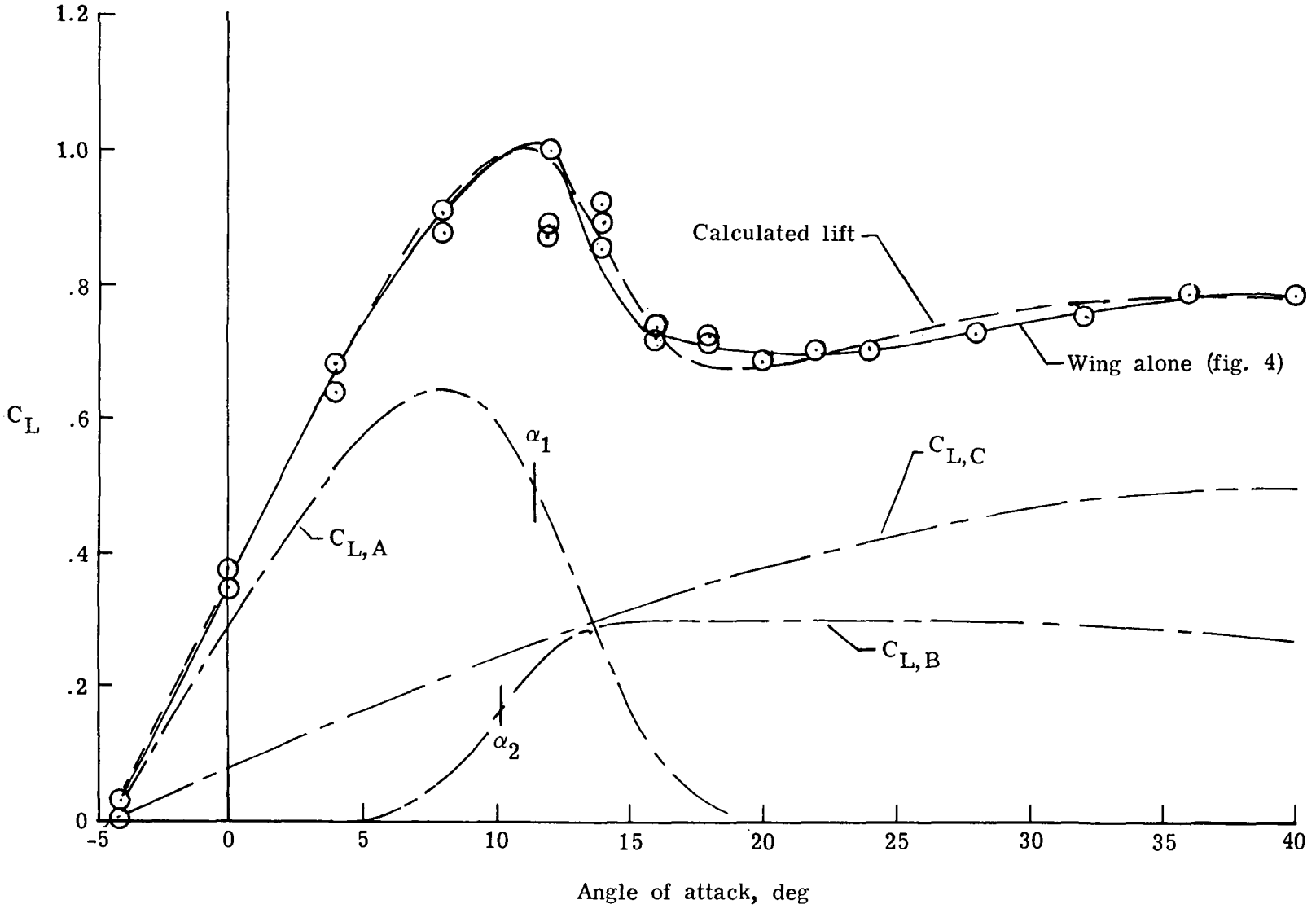


Figure 8.- Comparison of calculated lift and lift components with calculated wing-alone lift from data presented in figure 4. (For clarity, additional data points shown here were deleted from fig. 4.)

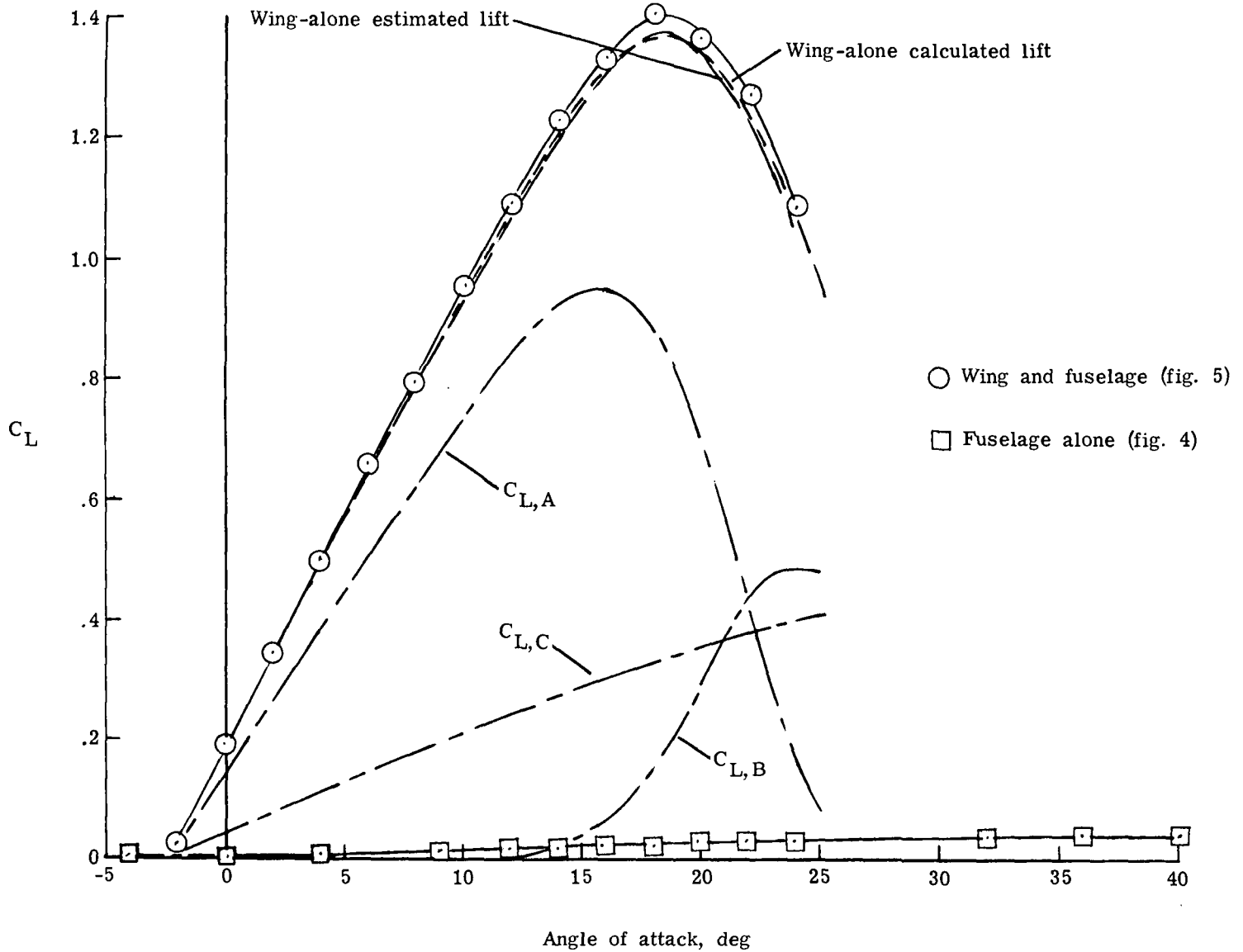


Figure 9.- Comparison of calculated lift and lift components with lift from data presented in figures 4 and 5.

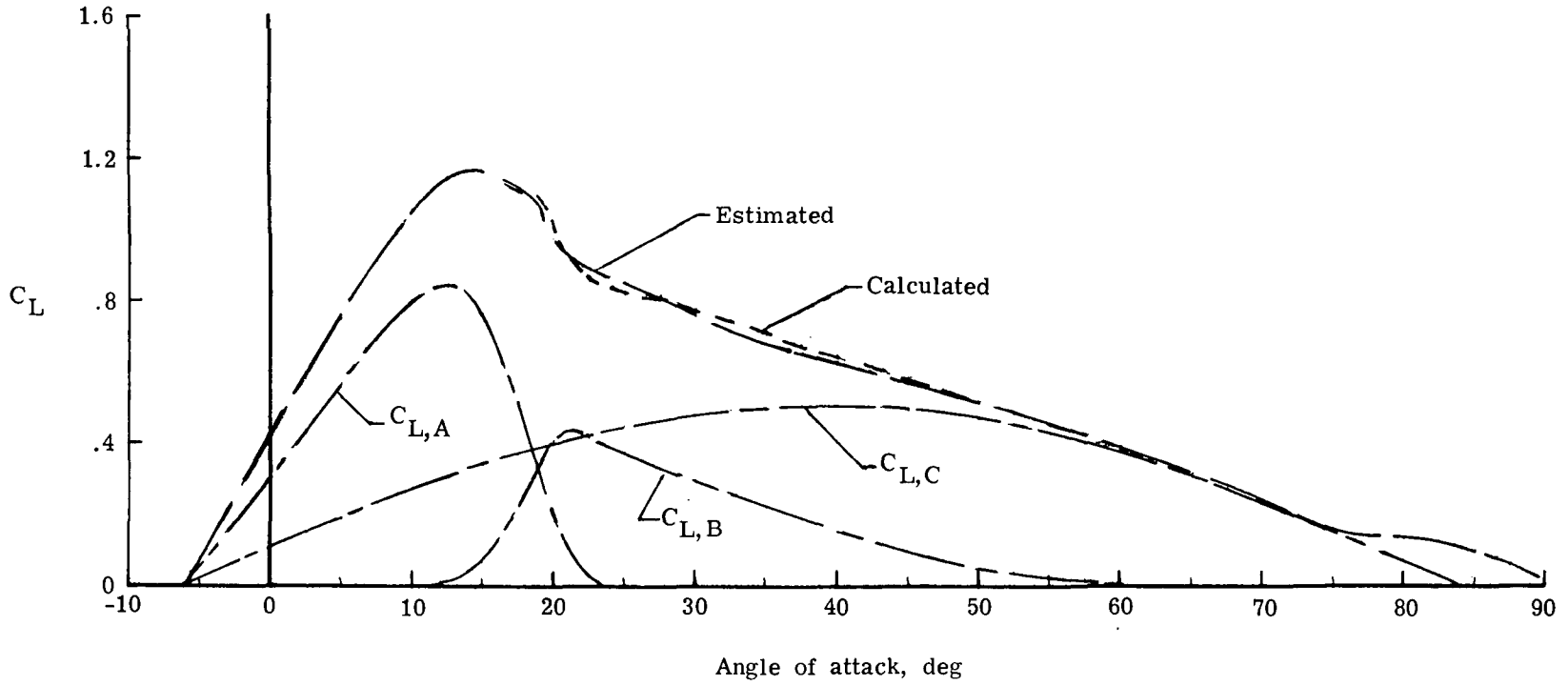


(a) $N_{Re} = 3.4 \times 10^6$; NACA $64_2$-415 airfoil.

Figure 10.- Comparison of calculated wing-alone lift and lift components with estimated lift derived from data presented in figure 6.

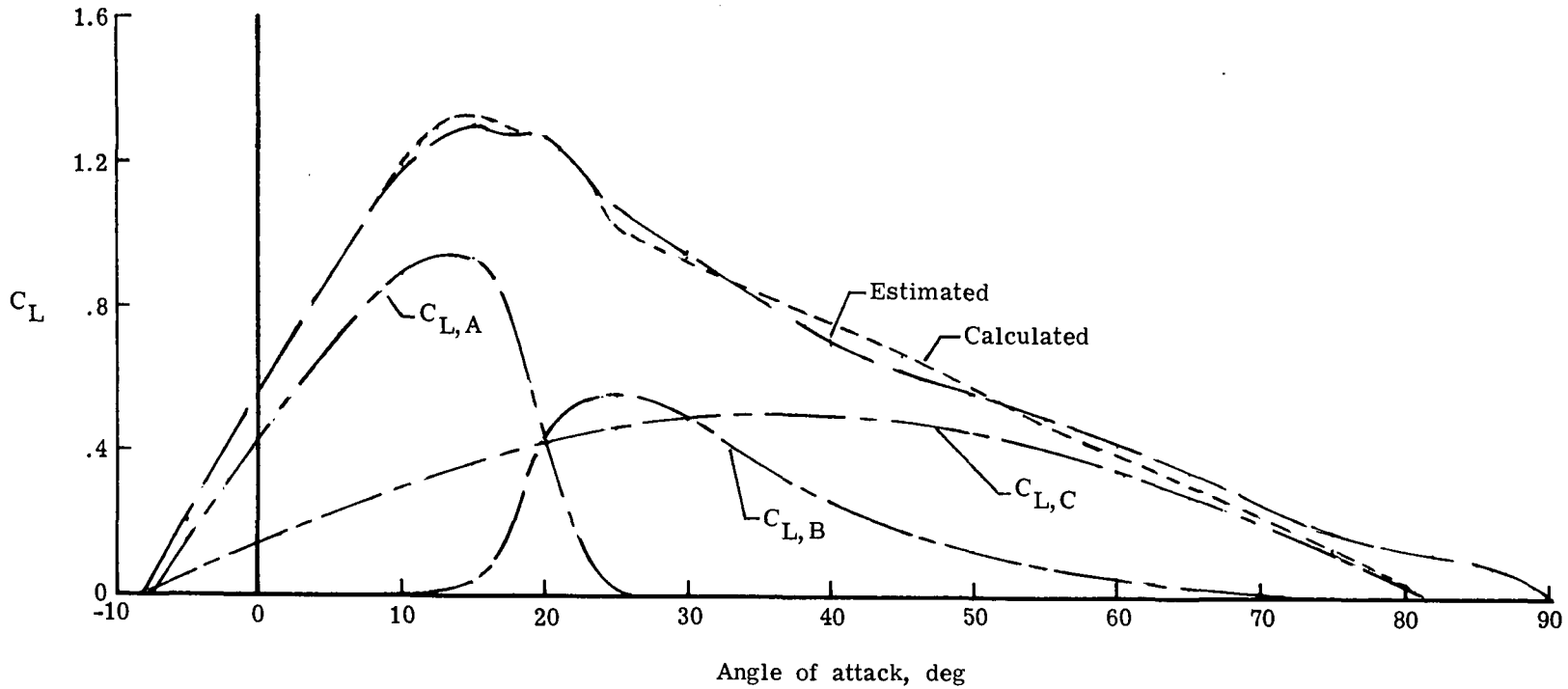


(b) $N_{Re} = 3.4 \times 10^6$; drooped leading edge.

Figure 10.- Continued.

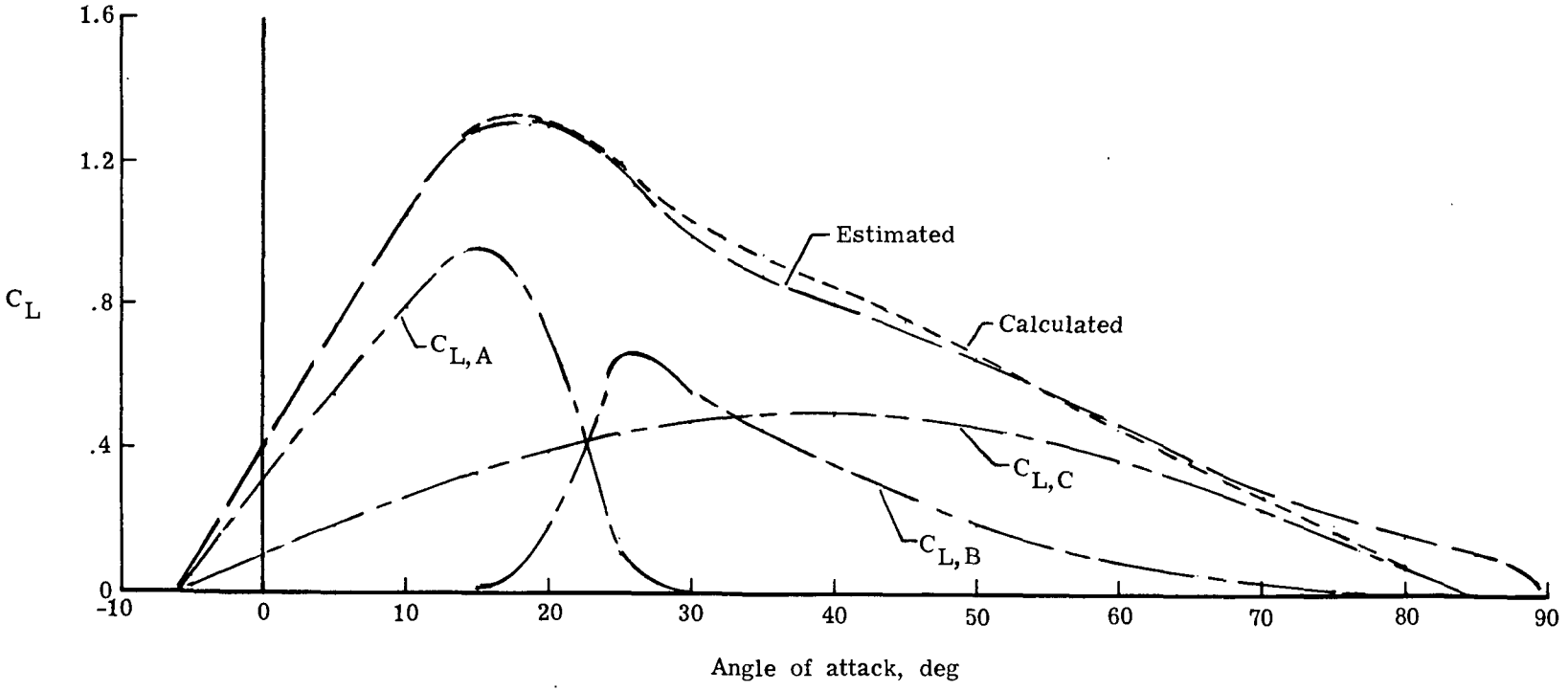


(c) $N_{Re} = 3.4 \times 10^6$; NASA GAW-1 airfoil.

Figure 10.- Concluded.

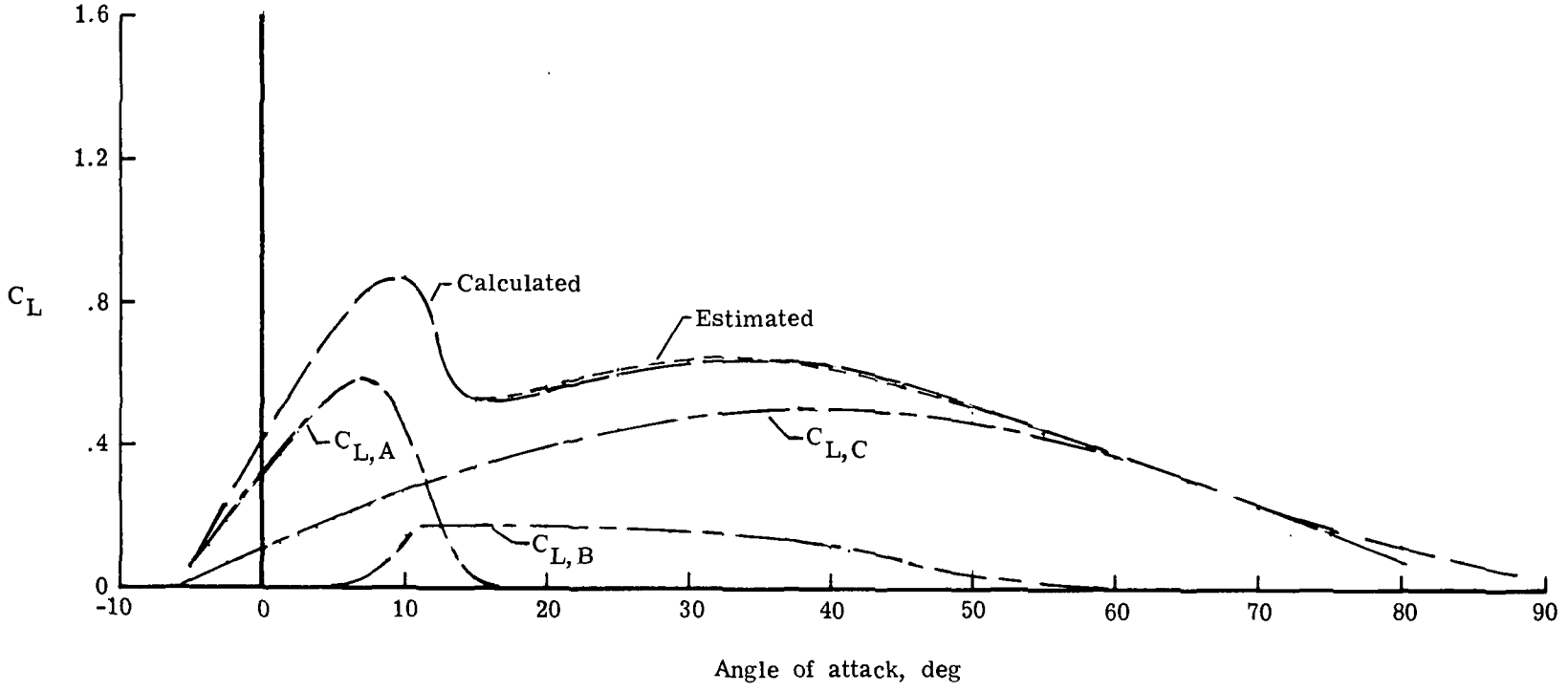


(a) $N_{Re} = 0.3 \times 10^6$; NACA $64_2$-415 airfoil.

Figure 11.- Comparison of calculated wing-alone lift and lift components with estimated lift derived from data presented in figure 7.

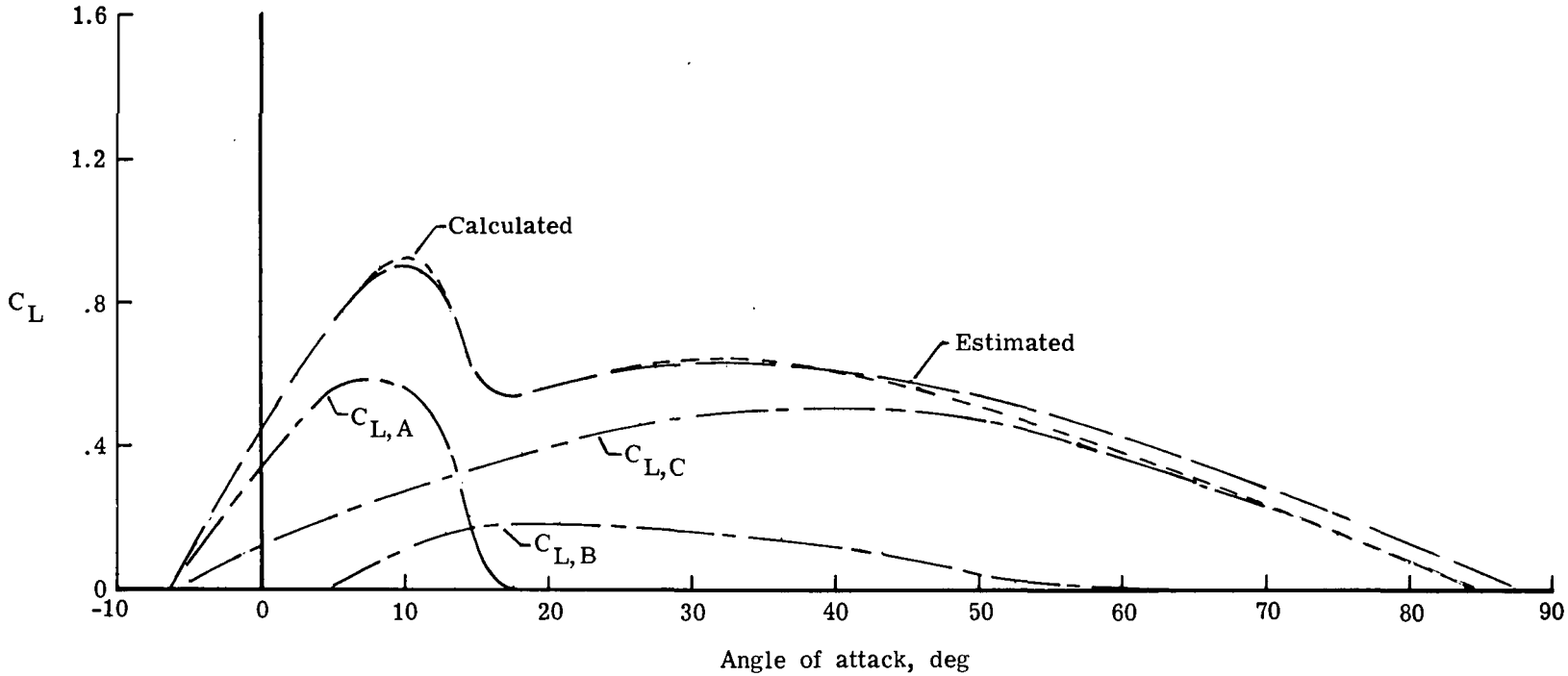


(b) $N_{Re} = 0.6 \times 10^6$; NACA $64_2$-415 airfoil.

Figure 11.- Continued.

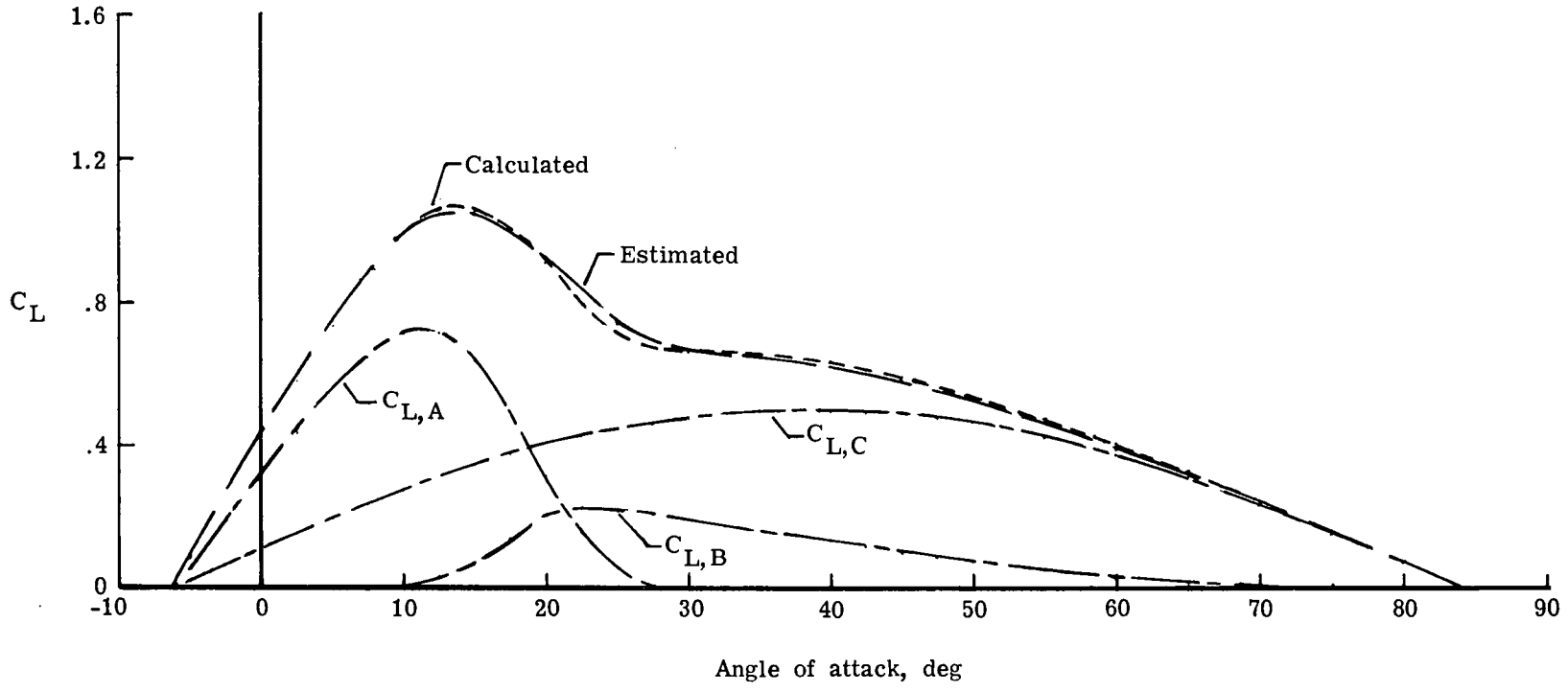


(c) $N_{Re} = 1.7 \times 10^6$; NACA $64_2$-415 airfoil.

Figure 11.- Continued.

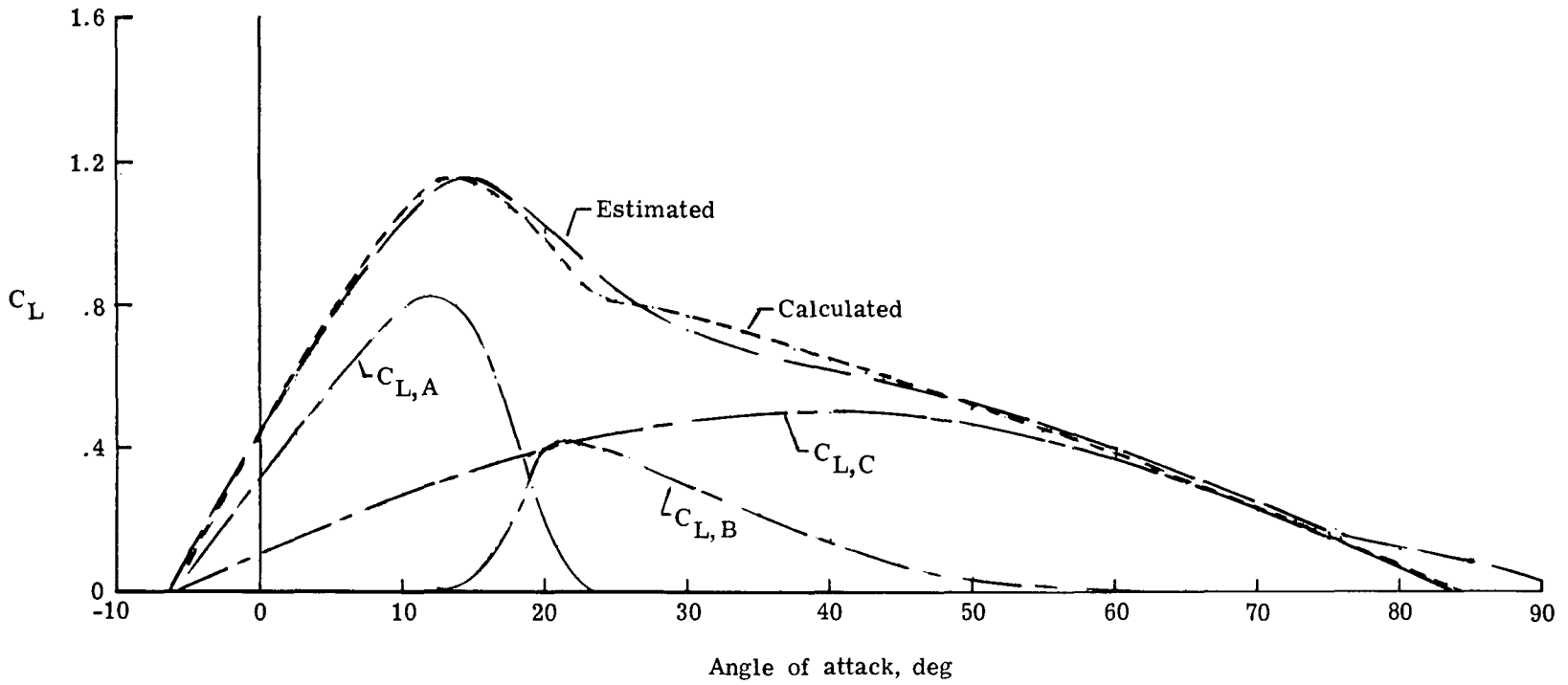


(d) $N_{Re} = 2.7 \times 10^6$; NACA $64_2$-415 airfoil.

Figure 11.- Concluded.

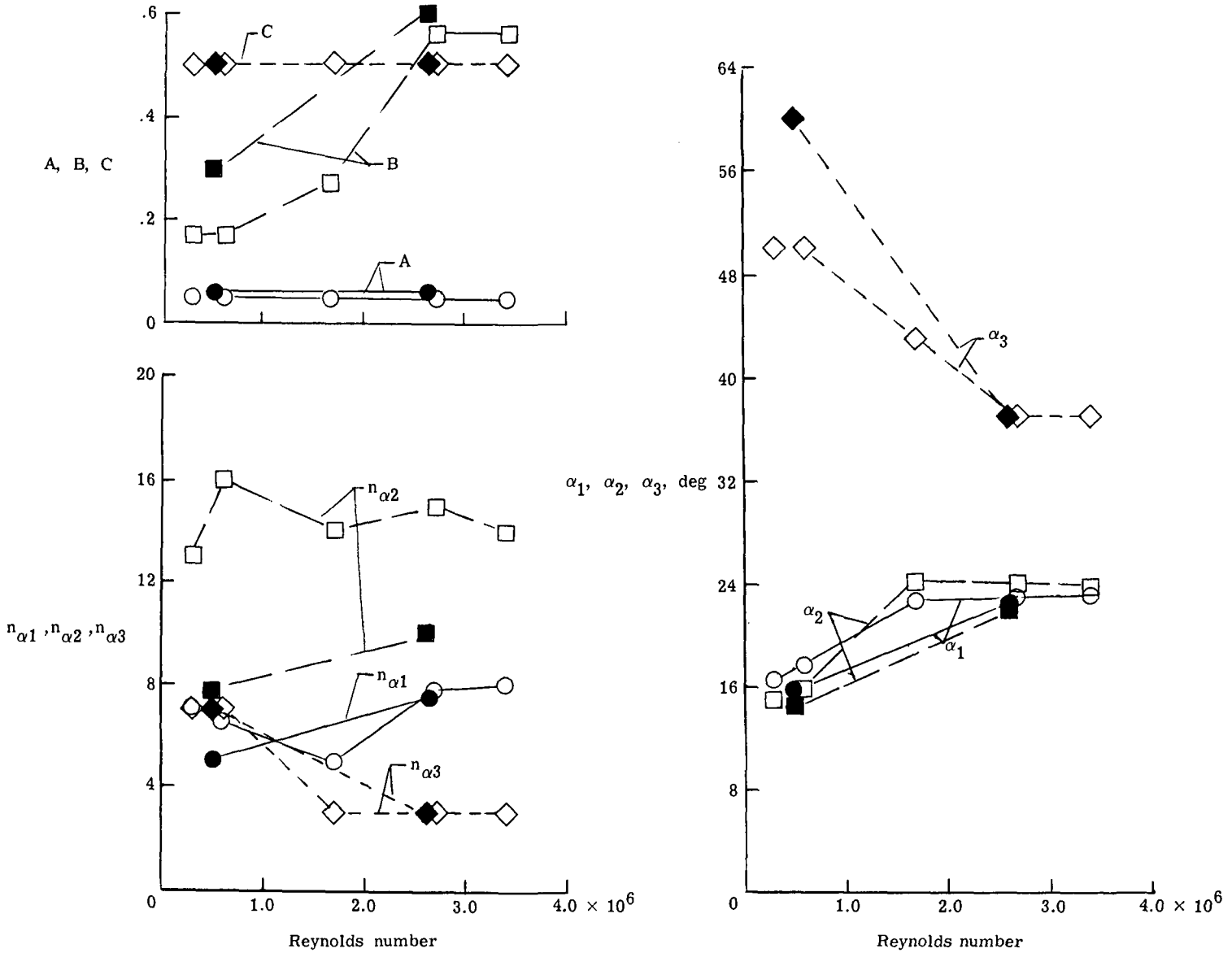


Figure 12.- Variation of coefficient values from table I with Reynolds number for low-wing model (open symbols) and high-wing model (solid symbols).

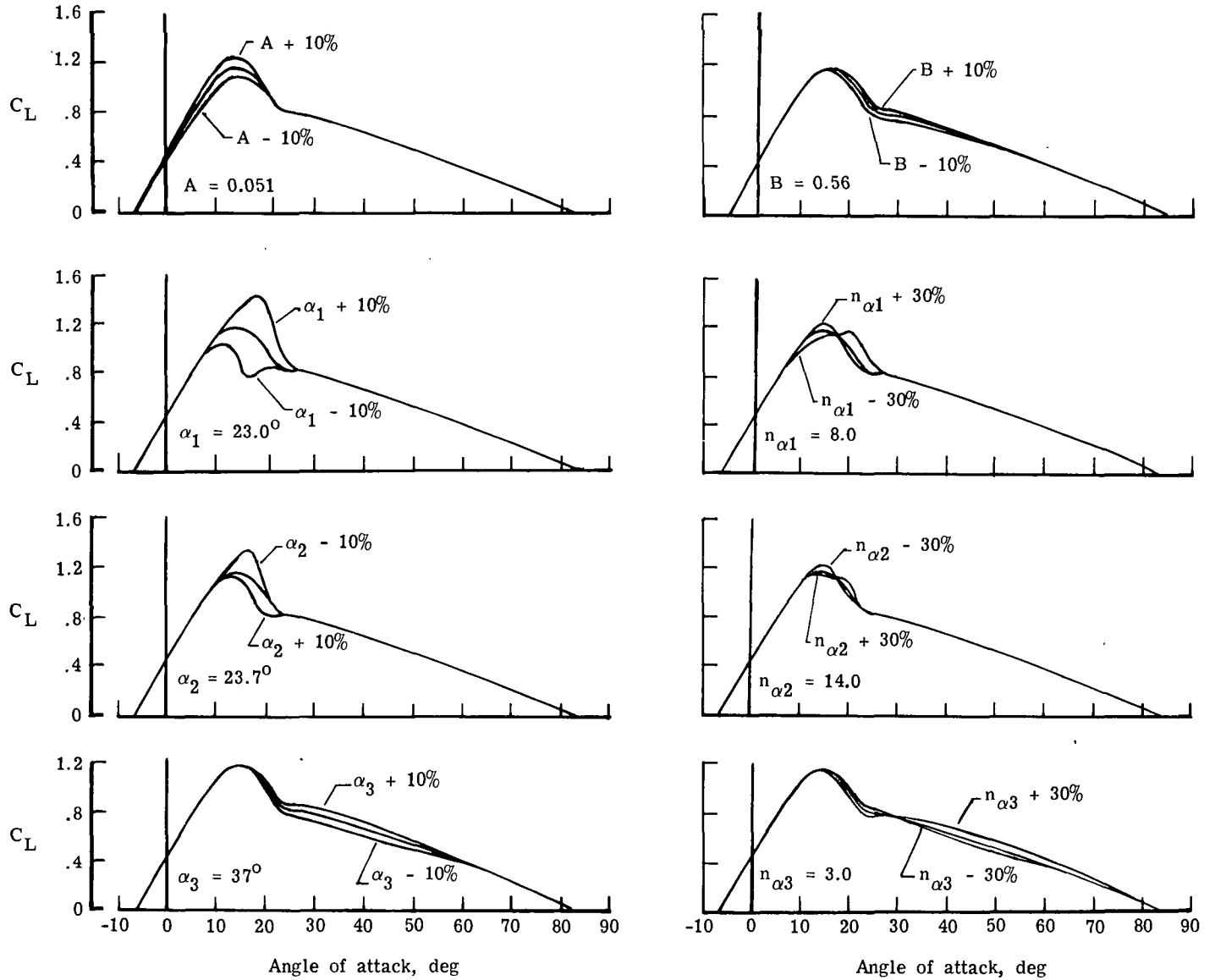


Figure 13.- Effects of calculated lift of variations in values of lift coefficients from equation (8).

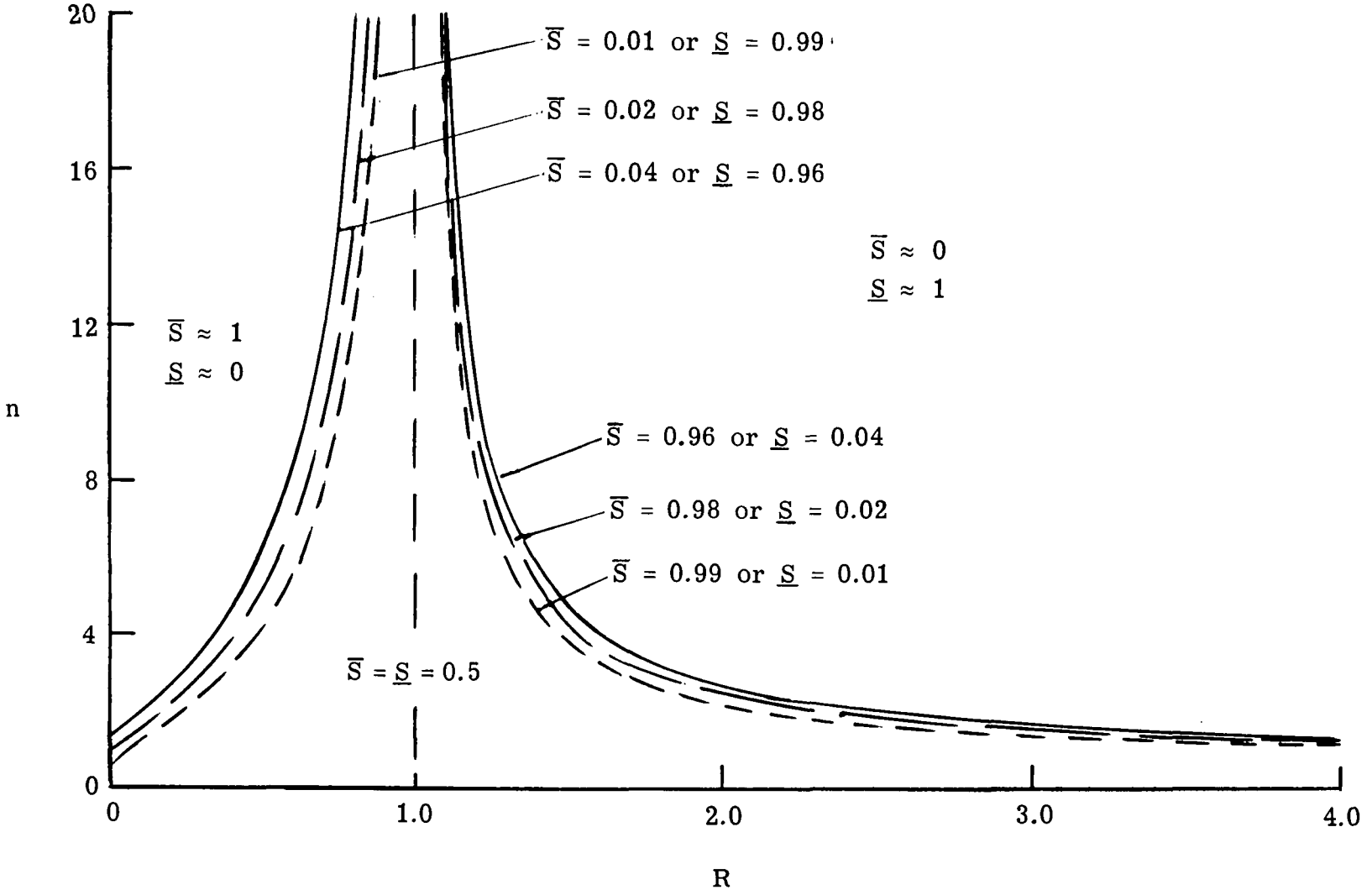


Figure 14.- Boundary plot of R and n for which $\bar{S}$ or $\underline{S}$ will be within 0.01, 0.02, or 0.04 of the values 0 or 1. (Regions outside two sets of curves indicate combinations of R- and n-values for which $\bar{S}$ or $\underline{S}$ can be preset to either 0 or 1.

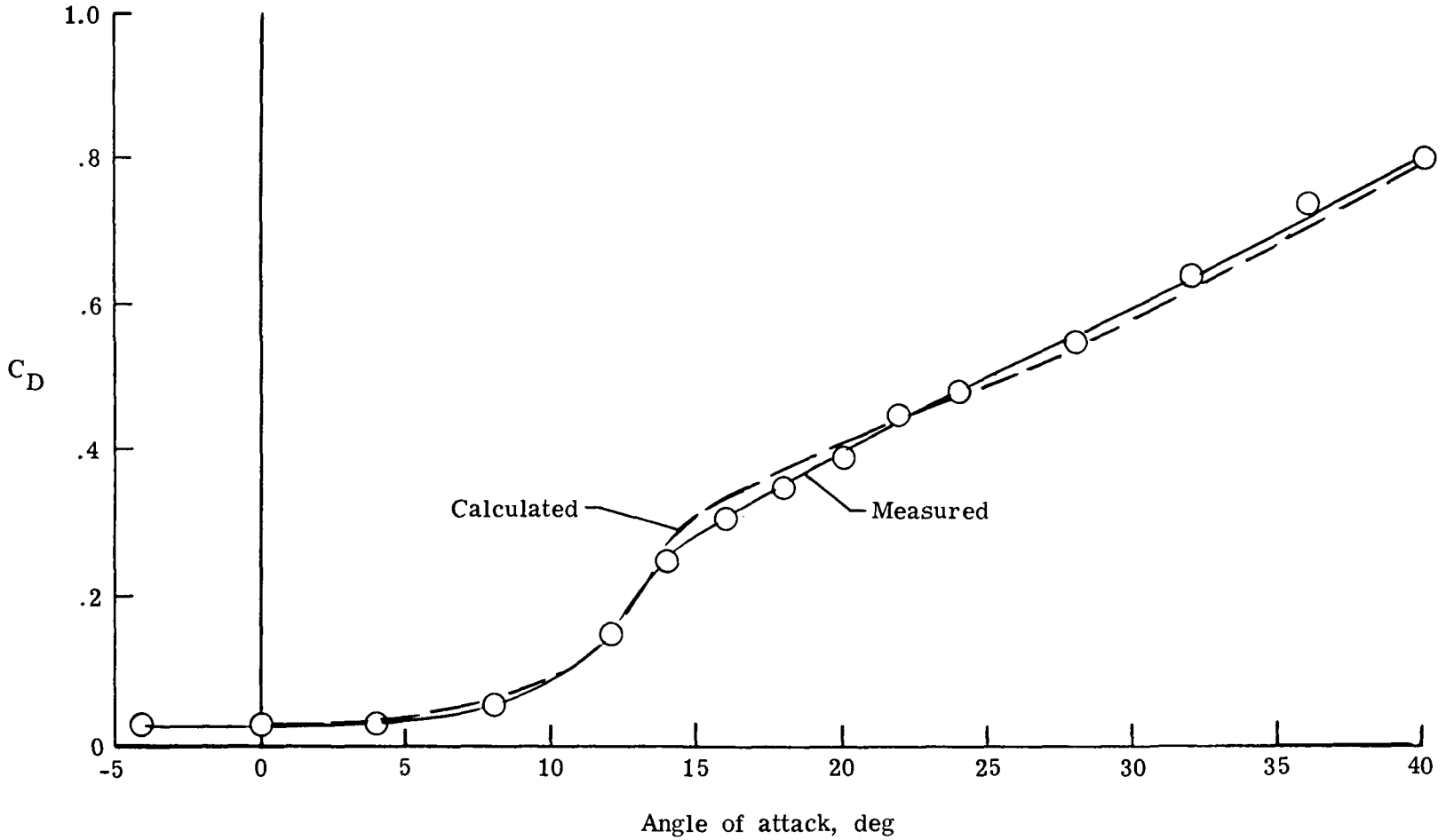


Figure 15.- Variation of measured and calculated wing-fuselage drag for angles of attack of $-4^{\circ}$ to $40^{\circ}$.

| 1. Report No. | 2. Government Accession No. | 3. Recipient's Catalog No. |
|---|---|---|
| NASA TM-78737 | | |

| 4. Title and Subtitle | 5. Report Date |
|---|---|
| DEVELOPMENT OF A NONLINEAR SWITCHING FUNCTION AND ITS APPLICATION TO STATIC LIFT CHARACTERISTICS OF STRAIGHT WINGS | September 1978 |
| | 6. Performing Organization Code |

| 7. Author(s) | 8. Performing Organization Report No. |
|---|---|
| Donald E. Hewes | L-12270 |
| | 10. Work Unit No. |
| | 505-10-13-04 |

| 9. Performing Organization Name and Address | 11. Contract or Grant No. |
|---|---|
| NASA Langley Research Center<br>Hampton, VA 23665 | |
| | 13. Type of Report and Period Covered |
| 12. Sponsoring Agency Name and Address | Technical Memorandum |
| National Aeronautics and Space Administration<br>Washington, DC 20546 | 14. Sponsoring Agency Code |

15. Supplementary Notes

16. Abstract

A mathematical-modeling technique has been developed for the lift characteristics of straight wings throughout a very wide angle-of-attack range. The technique employs a mathematical switching function that facilitates the representation of the nonlinear aerodynamic characteristics in the partially and fully stalled regions and permits matching empirical data within ±4 percent of maximum values. Although specifically developed for use in modeling the lift characteristics, the technique appears to have other applications in both aerodynamic and nonaerodynamic fields.

| 17. Key Words (Suggested by Author(s)) | 18. Distribution Statement |
|---|---|
| Mathematical switching function<br>Nonlinear lift | Unclassified - Unlimited<br><br>Subject Category 02 |

| 19. Security Classif. (of this report) | 20. Security Classif. (of this page) | 21. No. of Pages | 22. Price* |
|---|---|---|---|
| Unclassified | Unclassified | 41 | $4.50 |

* For sale by the National Technical Information Service, Springfield, Virginia 22161

NASA-Langley, 1978

National Aeronautics and
Space Administration

Washington, D.C.
20546

Official Business
Penalty for Private Use, $300

THIRD-CLASS BULK RATE

Postage and Fees Paid
National Aeronautics and
Space Administration
NASA-451

U.S.MAIL

5 2 1U,A, 090878 S90844HU
MCDONNELL DOUGLAS CORP
ATTN: PUBLICATIONS GROUP PR 15246-A
P O BOX 516
ST LOUIS MO 63166

NASA

POSTMASTER: If Undeliverable (Section 158 Postal Manual) Do Not Return

~~27 FEB 790~~ RAY HERRING 380/336/600 10 SEP 79G

12 OD 10 OCT 1978